Supplementary information

Summary

List of figures

List of tables

Supplementary note 1: OSMOSE-MED end-to-end model

1. General structure

The ecological and fishing effects of the expansion of different Mediterranean MPA scenarios was simulated using the OSMOSE-MED end-to-end model **(1)** (Supplementary Figure 1. 1) composed of:

(1) A regional atmosphere-ocean coupled climate models, CNRM-RCSM4 (2), driven one-way by atmosphere and ocean lateral boundary conditions extracted from the general circulation model CNRM-CM5 (3);

(2) A regional biogeochemistry model, Eco3M-S (4), which represents carbon, nitrogen, phosphorus and silica cycles at high-resolution to simulate the dynamics of seven key planktonic functional types in the Mediterranean Sea;

(3) A multi-species age and size-structured stochastic model, OSMOSE (1), which simulates at a medium spatio-temporal resolution (regular grid of 6229 cells of 20 x 20 km2; 15-day time step) the life cycle of 100 marine species (85 fish, 5 cephalopods and 10 crustaceans), representing about 85% of the total declared catches in the Mediterranean Sea, for the period 2006-2013.

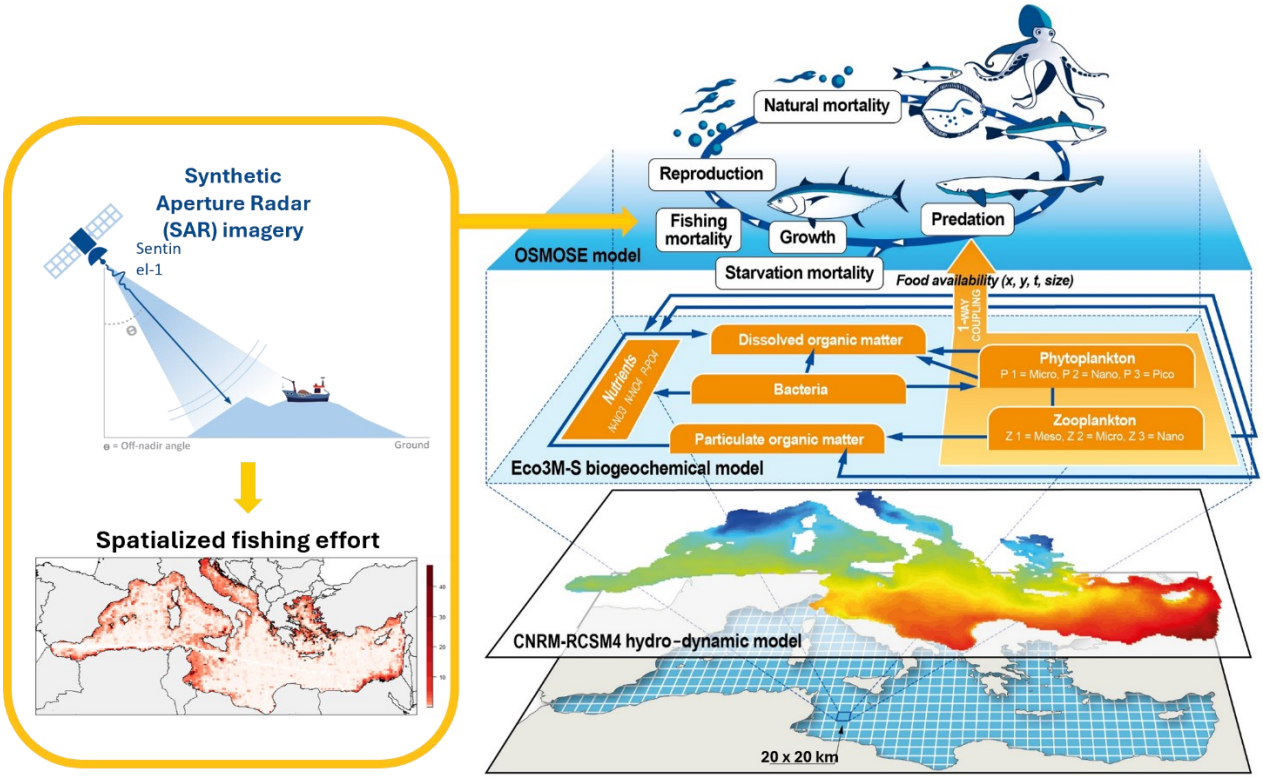

Supplementary Figure 1. 1: Conceptual representation of the OSMOSE-MED modelling chain (adapted from (1))

2. The low trophic level model CNRM-RCSM4 / Eco3M-S

Eco3M-S is a biogeochemical model that represents carbon, nitrogen, phosphorus and silica cycles at high resolution to simulate the dynamics of seven key planktonic functional types, consisting of three size classes of phytoplankton (pico-, nano- and micro-phytoplankton), three size classes of zooplankton (nano-, micro- and meso-zooplankton) and heterotrophic bacteria as decomposers, responsible for the remineralization of dissolved organic matter (4). The representation of the heterotrophic processes was based on the models developed by (5, 6). All features, formulations and parameterization of biogeochemical processes integrated in the mechanistic Eco3M-S model are described in detail in (4, 7, 8).

In addition to these 7 low-trophic level groups, a benthos compartment was added as it represents part of the diet of several species included in the OSMOSE-MED model. Size range and trophic level parameters, as well as biomass levels that were assumed to be uniform across the Mediterranean Sea, were derived from the Ecopath model of (9), but life cycle dynamics were not modelled.

The CNRM-RCMS4 - Eco3M-S low trophic level model was used to force the OSMOSE model through offline one-way coupling.

3. The high trophic level model OSMOSE

3.1. The OSMOSE model

OSMOSE is a size-based multispecies trophic model that zooms in on the higher trophic levels of marine ecosystems, focusing on fish and macroinvertebrate species. The model is designed with a spatially explicit approach, aiming to capture the full life cycle of interacting marine species. It simulates key life cycle processes, such as growth, predation, reproduction, natural and starvation mortality, and fishing mortality, from the initial stage of eggs to adult fish. To overcome the computational challenges of time and memory limitations, OSMOSE relies on 'super-individuals', rather than true individuals, that act as proxies for schools of fish. Fish schools are defined as groups of individuals of identical age, length, diet, and spatial position, interacting within a two-dimensional grid through predation (10).

OSMOSE incorporates species-specific spatial distribution maps that may vary between years, seasons, or ontogenetic stages. Its fundamental assumptions about predation lead to the emergence of complex trophic interactions. Unlike other trophic models, such as Ecopath with Ecosim (11), OSMOSE does not rely on pre-established trophic interactions between species. Each fish in

OSMOSE has the potential to be a predator or prey, regardless of its taxonomy, based on size compatibility (10, 12). The model introduces maximum and minimum predator/prey size ratios to govern predator-prey interactions (13). To introduce a vertical dimension to the food web, accessibility coefficients are defined in a prey-predator accessibility matrix, which reflects potential mismatches or overlaps between the vertical distributions and/or refugia of species, such that part of a school of fish may remain inaccessible to predators.

At each time step, OSMOSE calculates a predation efficiency rate for each school of fish, representing the food biomass ingested within that time step relative to the maximum ingestion rate. This rate in turn determines growth, starvation and reproduction rates. The growth and mortality functions in OSMOSE are deterministic, with stochasticity arising mainly from the movement of fish schools within their habitat and the order in which schools interact through predation. More detailed information can be found at https://documentation.osmose-model.org/.

3.2. Application to the Mediterranean Sea

OSMOSE was applied to the entire Mediterranean Sea (from approximately 26.9°N to 46.3°N in latitude and 5.6°W to 253 36.1°E in longitude) for the period 2006-2013. The resulting OSMOSE-MED model represents 100 species: 85 fish, 10 crustaceans and 5 cephalopods (see *Supplementary Table 6.1* for list of species).

3.2.1. Species distribution

A niche modeling approach, based on environmental data (temperature and salinity), was used to generate species distribution maps within the Mediterranean Sea to drive the spatial distribution of species in the model. Species occurrence information was compiled and integrated from various sources, including the Ocean Biogeographic Information System (OBIS: www.iobis.org), the Global Biodiversity Information Facility (GBIF: www.gbif.org), the Food and Agriculture Organization's Geonetwork portal (www.fao.org/geonetwork), and the FishMed database atlas of fishes of the North Atlantic and Mediterranean (14).

Environmental predictor variables for climate data were obtained from the World Ocean Atlas 2013 version 2 (https://www.nodc.noaa.gov/OC5/woa13/woa13data.html). To account for the vertical distribution of species in the water column, six environmental metrics were derived from monthly temperature and salinity climatologies. These metrics included mean sea surface temperature and salinity (0-50 m depth), mean vertical temperature and salinity (0-200m depth), and mean sea bottom

temperature and salinity (50 m - maximum bathymetric depth). These metrics were used to model bioclimatic envelopes for each species.

Eight climate suitability models were used to model current species distributions, including generalized linear models, generalized additive models, classification tree analysis, boosted regression trees, random forests, multivariate adaptive regression splines, artificial neural networks and flexible discriminant analysis. These models were embedded in the BIOMOD2 R package (15).

As the OBIS and GBIF databases only provide occurrence data on a global scale, pseudo-absences (PAs) were generated to build reliable species distribution models (16). PAs were randomly selected outside the appropriate area of the surface range envelope model, and their number was double that of the occurrence data. These PAs were weighted equally with the occurrence points during the fitting process.

The accuracy of the final distribution maps was assessed using the True Skill Statistic (17), which is a combined measure of model sensitivity (proportion of correctly predicted presences) and specificity (proportion of correctly predicted absences).

The whole modelling process is described in (18).

3.2.2. Calibration and model evaluation

OSMOSE-MED was calibrated using the R package *Calibrar* (19), designed for the calibration of complex stochastic models. The calibration process estimated unknown parameters, such as larval mortality rates, availability coefficients, and fishing mortality, while constraining predicted biomass and catch of high trophic level (HTL) species within realistic ranges by comparing the model to observed data using maximum likelihood objective functions (20). The mean of reported fishery landings from the United Nations Food and Agriculture Organization General Fisheries Commission for the Mediterranean (FAO-GFCM) database and of reconstructed catches from the Sea Around Us (SAU) project (21) for the period 2006-2013 were used as minimum and maximum bounds for catch data for all species, except for tuna and swordfish, for which data were extracted from the International Commission of Conservation of Atlantic Tuna [i](ICCAT) statistics database. When available and realistic, cumulative biomass from stock assessments was used for biomass estimates, except for *Thunnus thynnus* and *Thunnus alalunga*, which were based on expert knowledge (Fromentin J.M. and Winker H., pers. comm.). Biomass estimates for all species were assumed to lie

between FAO reported catches and FAO/SAU average catches, considering an exploitation rate of 15%.

The biomass model outputs were evaluated with independent data from the International Mediterranean Bottom Trawl Survey (MEDITS) for the period 2006-2013, which were not used for the calibration and parametrization of the model, nor for the generation of the species distribution maps (1). The mean trophic level of each species was compared for each species with data from the FishMed database (14), the Mediterranean-scale Ecopath model (9) and a review of the feeding habits and trophic levels of 148 fish species (22, 23). To test whether the size-based predation hypothesis led to consistent diets, we compared the adult diets of the four most important species in terms of catch volume or value in the Mediterranean, with those derived from the Ecopath model (9), based on the available literature and empirical data.

The calibration process and the confrontation of OSMOSE-MED outputs to data are described in (1).

Supplementary note 2: Spatialization of the fishing effort across the Mediterranean basin

Given the composition of the Mediterranean fishing fleet (ca. 83% of small-scale vessels under 12 m) (24), the exclusive use of Automatic Identification System (AIS) data to estimate fishing effort at whole-basin scale introduces a strong bias because: (1) AIS transmission is only mandatory for vessels over 15 m in length in the European Union, (2) AIS data omit illegal, unreported and unregulated (IUU) fishing, which is widespread in the Mediterranean Sea (25), although its nature and extent are still not well documented (26), and (3) AIS data gaps due to signal interferences or low coverage are pronounced in the southeastern part of the basin, particularly along the Egyptian coast, where data are also more scarce. Synthetic Aperture Radar (SAR) satellite imagery appeared as a more suitable option to map fishing effort in this region. Not critically affected by weather conditions (e.g., cloud coverage) and day-night cycles, SAR satellites provide high-resolution images which can allow to detect ships above 10 m in length and therefore appear as a suitable solution to detect vessel position in real-time (27). Following (27), we acquired 14,278 Ground Range Detected High-Resolution (i.e., 10 meters per pixel) images from Sentinel-1A and Sentinel-1B, the SAR satellite constellation of the European Union's Copernicus program for Earth Observation, operated by the European Space Agency from the Alaska Satellite Facility platform (28) covering the extent of the entire Mediterranean basin during the period 1 January – 31 December 2019.

Vessels were detected using the Search for Unidentified Maritime Objects (SUMO) algorithm developed by the European Joint Research Center (29). SUMO is a pixel-based constant false alarm rate detector that uses multiple detection thresholds to distinguish ships from sea clutter (30). We applied a 100 meter buffer around the land mask to avoid coastal clutter. SUMO was run in fully automatic mode to perform target detection, and detection threshold adjustments were set to 2.3 and 1.3 for co-polarization (VV) and cross-polarization (VH), respectively, which appeared to be the best compromise to deal with the irregular distribution of the radar backscatter over a target (31). The storage and processing of the data was technically challenging (approximately 40 terabytes of images), so the images had to be downloaded, processed and erased in blocks.

SUMO calculates a reliability factor to distinguish between likely real targets and likely false alarms. To minimize the number of false positives, we followed the methodology developed by (32) and deleted all false alarms and images with 95% more detections than the average image. In a

conservative approach, detections in major transport shipping corridors provided by the dataset of **(33)** at 1 km^2 resolution were also omitted, as we assumed that fishing vessels would represent only a small fraction of the total detections in such areas. To account for information loss, we defined cells in major shipping corridors if the number of detections was equal to or greater than 20 (Supplementary Figure 2. 1). Similarly, we deleted all detections found within a 10 meter buffer of offshore installations provided by the Emodnet human activities platform (https://www.emodnet-humanactivities.eu).

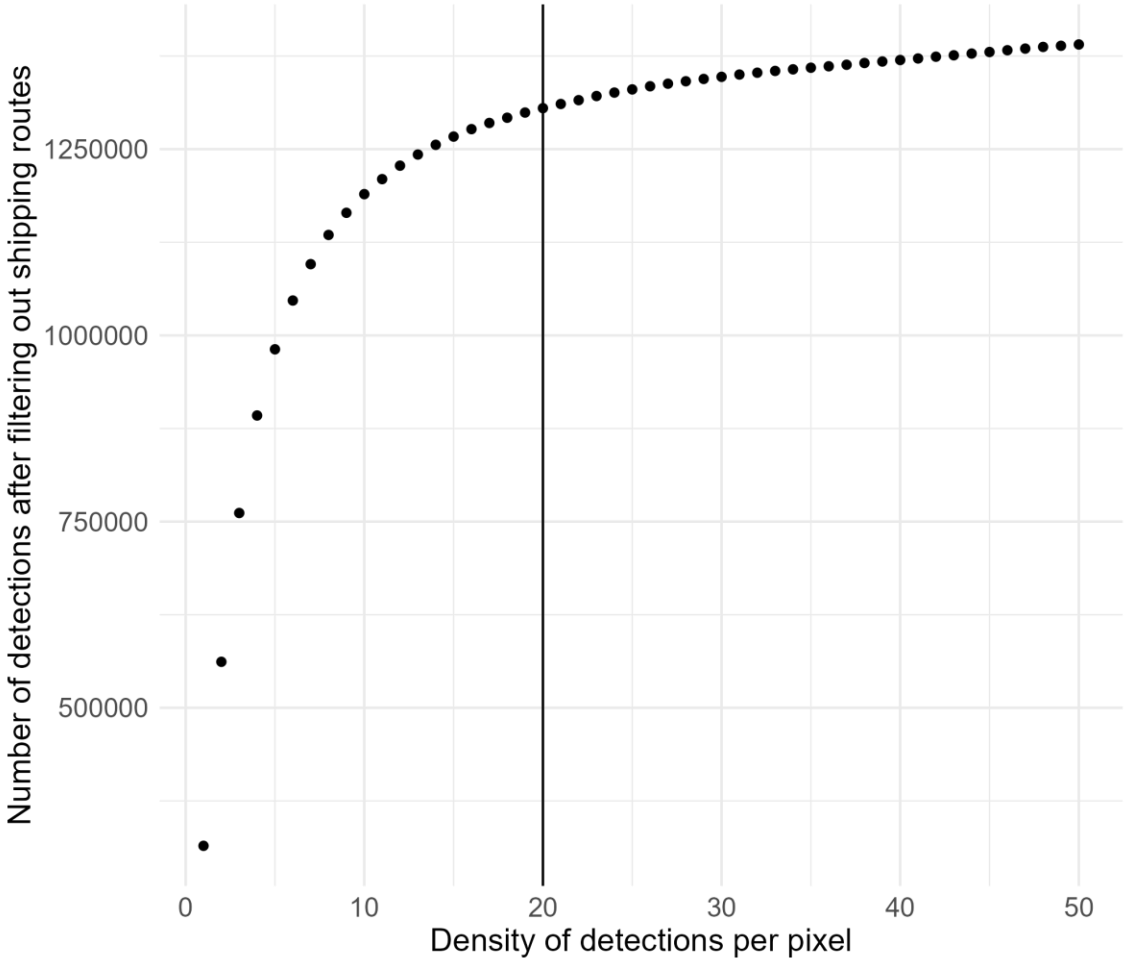

*Supplementary Figure 2. 1: Cumulated ship detections per pixel (km^2) according to the filter threshold used, i.e. density of boats per pixel (methodology from **(32)**). We chose to filter out pixels containing over 20 detections, which seemed the best compromise between the amount of information lost and accuracy of the information kept.*

Another known important source of false detections are images affected by radio frequency interference (RFI) **(27)**. However, due to the very important number of images, we were not able to

exclude all RFI-labelled images. Instead, we decided to manually remove only images located in areas with an unusually high density of detections in linear patterns. The eastern Mediterranean Sea off the coast of Israel and Egypt (between 30.7° and 34.7° in latitude and between 29.8° and 36° in longitude) and the Strait of Sicily (between 31° and 37° in latitude and between 11° and 18° in longitude) were identified as RFI hotspots (Supplementary Figure 2. 2), and a total of 102 images in these areas were discarded.

According to the SUMO estimate of detected vessel length, vessels ranged from 10 m to 999 m. This maximum length is unrealistic for fishing vessels and vessels in general. In order to obtain a better estimate of the number of fishing vessels, we filtered out all detections with an estimated length greater than 60 m, which corresponds to the maximum size of fishing fleets in the Mediterranean Sea according to fishing effort data from Global Fishing Watch (https://globalfishingwatch.org/datasets-and-code/), which uses AIS and two convolutional neural networks to identify vessel characteristics and detect AIS positions indicative of fishing activity **(34)**. Despite these precautions, our dataset may still contain non-fishing vessels, especially in regions with high tourism activity where recreational or commercial vessels unrelated to fishing are prevalent, as SAR imagery does not give any information on the activity of the potential vessel detected.

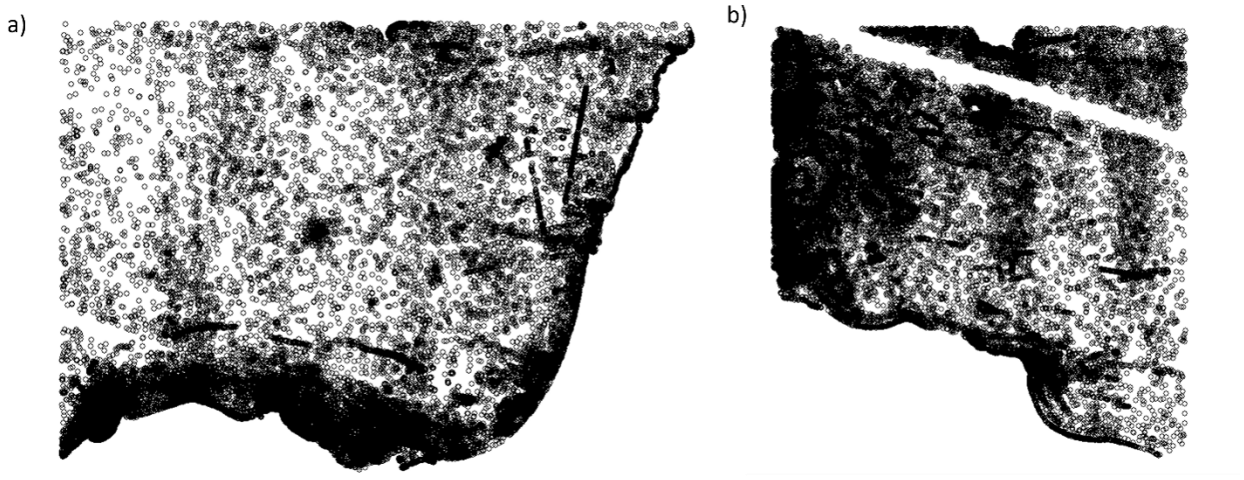

Supplementary Figure 2. 2: Detections in the eastern Mediterranean Sea (a) and in the Strait of Sicily (b). Black lines are due to radio-frequency interferences.

Finally, we noticed that the revisit period of each satellite is not uniform across the Mediterranean Sea, with some areas being imaged more frequently due to overlap in neighboring swaths, leading to a

bias in the number of detections (Supplementary Figure 2. 3). To minimize this bias, we corrected the number of detections per OSMOSE-MED grid cell according to the number of times each cell was imaged from 1 January to 12 January 2019. A 12-day time period was chosen because the Sentinel-1 satellites have a 12-day repeat cycle (Supplementary Figure 2. 4). The different processing steps with the associated number of detections and number of images are summarized in *Supplementary Table 2. 1*.

Supplementary Table 2. 1: Number of detections and images used to create the Mediterranean fishing effort map used in the OSMOSE-MED model.

Data processing steps	Number of detections	Number of images
All Sentinel 1A & 1B 2019 images	1,698,952	14,278
Without false alarms	1,425,526	14,129
Not in main commercial shipping lanes	1,305,051	14,129
Under 60 m in length	472,067	13,765
Not within a 10 m buffer of offshore platforms	471,881	13,765
Not in high density RFI images	463,672	13,663
Detections used to create effort map	**463,672**	**13,663**

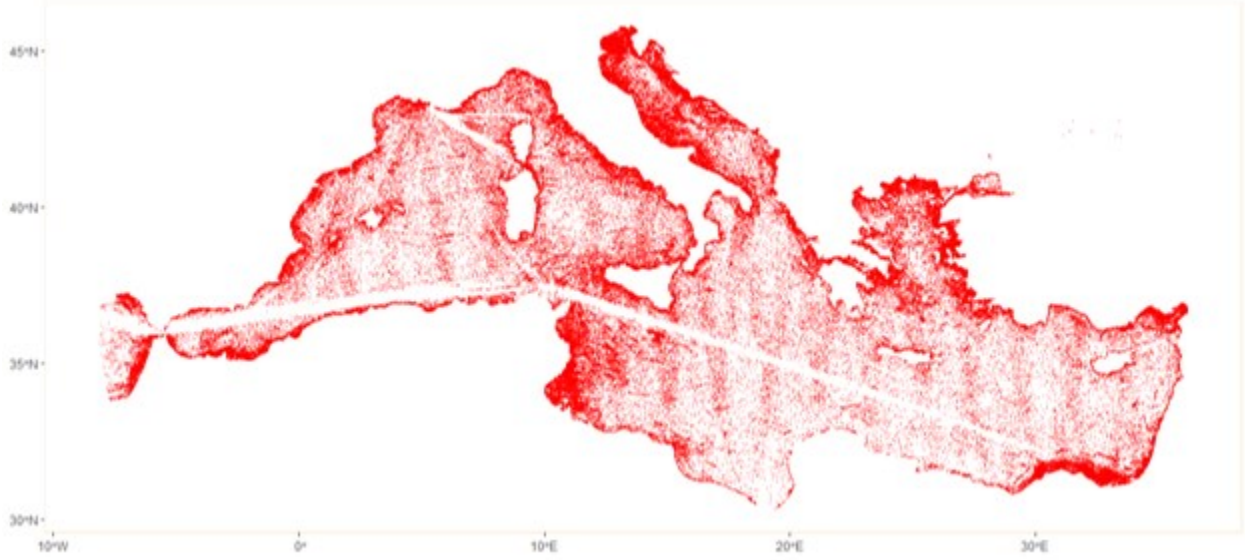

Supplementary Figure 2. 3: Fishing effort measured as the cumulative number of vessels operating in the Mediterranean Sea in 2019. Each red dot represents a potential fishing vessel detected from SAR imagery using the SUMO algorithm. Only detections of vessels under 60 m were retained. Offshore platforms and commercial shipping lanes have been filtered out. Images affected by RFI off the Israeli and the Egyptian coast and in the Strait of Sicily were excluded.

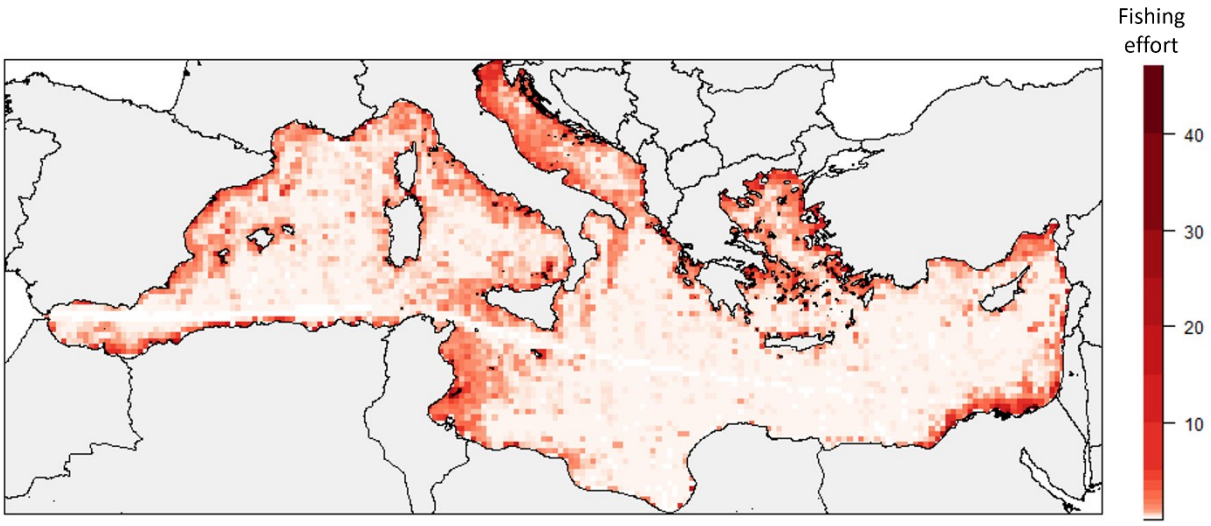

Supplementary Figure 2. 4: Fishing effort distribution in the Mediterranean Sea, obtained via SAR imagery. Values are expressed as number of vessels per km² standardized over the entire Mediterranean Sea.

Supplementary note 3: Fishing effort displacement scenarios

Three fishing effort redistribution strategies have been modelled, with f_{in} and f'_{in} the fishing effort within an MPA before and after implementation respectively, f_{out} and f'_{out} the fishing effort outside an MPA before and after implementation.

1. Fishing-the-line redistribution scenario

$\forall\, j \in \{1, \dots, m\} \quad m = number\ of\ MPAs\ in\ the\ Mediterranean\ Sea$

$\forall\, i \in \{1, \dots, n_j\} \quad n_j = number\ of\ cells\ inside\ of\ MPA_j$

$\forall\, b \in \{1, \dots, s_j\} \quad s_j = number\ of\ cells\ on\ the\ border\ of\ MPA_j$

$$f'_{in_{i_j}} = 0$$

$$f'_{b_j} = f_{b_j} + \frac{1}{s_j} * \sum_i^{n_j} f_{in_{i_j}}$$

2. Uniform redistribution by GFCM geographical sub-area (GSA)

$\forall\, j \in \{1, \dots, m\} \quad m = \text{number of GSAs in the Mediterranean Sea}$

$\forall\, i \in \{1, \dots, n_j\} \quad n_j = \text{number of cells in } GSA_j,\ nMPA_j = \text{number of MPA cells in } GSA_j$

$$f'_{in_{i_j}} = 0$$

$$f'_{out_{i_j}} = f_{out_{i_j}} + \frac{1}{(n_j - nMPA_j)} * \sum_{i}^{n_j} f_{in_{i_j}}$$

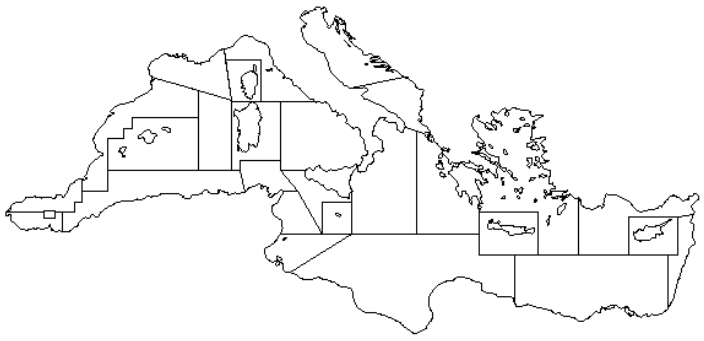

Supplementary Figure 3. 1: GFCM geographical sub-areas of the Mediterranean Sea.

3. Proportional redistribution by GSA relative to effort before reserve establishment

$\forall\, j \in \{1, \dots, m\} \quad m = \text{number of GSAs in the Mediterranean Sea}$

$\forall\, i \in \{1, \dots, n_j\} \quad n_j = \text{number of cells in } GSA_j$

$$f'_{in_{i_j}} = 0$$

$$f'_{out_{i_j}} = f_{out_{i_j}} + \frac{f_{out_{i_j}}}{\sum_{i}^{n_j} f_{out_{i_j}}} * \sum_{i}^{n_j} f_{in_{i_j}}$$

Supplementary note 4: MPA network scenarios

1. Scenario summary description

We compared 6 different large-scale no-take MPA network configurations, which we expanded to a coverage of 30% by steps of 1% (Supplementary Figure 4. 1, Supplementary Table 4.1).

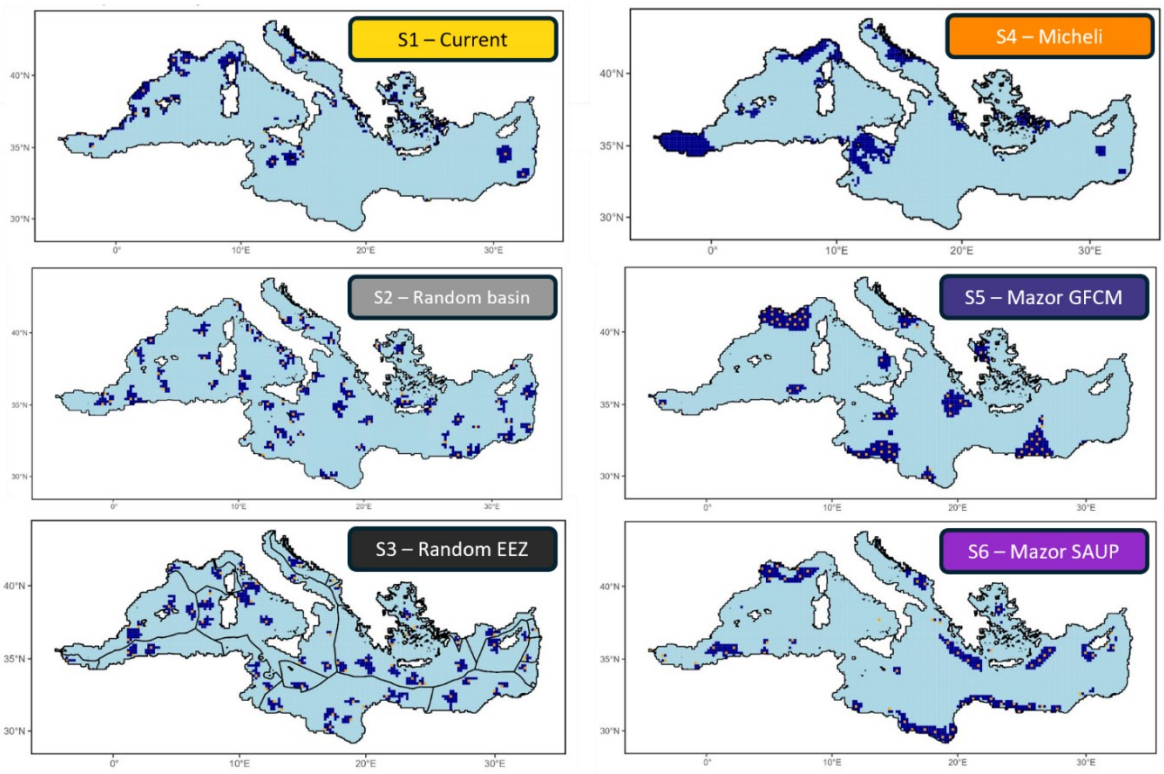

Supplementary Figure 4. 1: Tested no-take MPA network configurations for a 10% coverage (in dark blue). For scenarios S1-S3 and S5-S6, the location of the initial cells is represented in orange. See Supplementary Table 4.1 for a full description of the scenarios. Only one random S2 and one random S3 MPA networks are represented here (10 random S2 and 10 random S3 have been generated).

Supplementary Table 4. 1: Description of the 6 MPA network configurations tested. All MPA scenarios are seeded with 62 MPA cells (representing 1% of the total number of cells of OSMOSE-MED grid), forming an individual MPA patch. We defined MPA patches as one or more protected neighboring cells by queen neighborhood (8-neighbouring cells) entirely bounded by a border of unprotected cells. All MPA networks were expanded by steps of 1%, i.e. 62 new MPA cells by step. For all scenarios except S4-Micheli below 10% coverage, the expansion of MPA patches was done by randomized rook neighborhood, i.e. new MPA cells at each step were selected among the 4-neighbouring cells of each MPA patch.

#	Scenario name	Description	Implementation within OSMOSE-MED	Source
S1	Current	Expansion of the current MPA network in the Mediterranean Sea, made up of National MPAs, Natura 2000 sites and Fisheries Restricted Areas (FRAs).	62 initial cells placed at the barycenter of each MPA patch, consisting of cells that are more than 38% covered by an MPA, making up 62 MPA patches. The 38% threshold was set to obtain the number of OSMOSE-MED grid cells corresponding to the percentage coverage of the current MPA network used as baseline (see Supplementary Table 4. 1). MPAs were expanded through randomized rook neighborhood, with the condition (when possible) that each new MPA cell be located within the current MPA network (refer to section 1.1 for details).	This study
S2	Random basin	Random placement of MPAs across the Mediterranean Sea.	62 initial cells making up 62 MPA patches randomly distributed across the OSMOSE-MED sea grid. MPAs were expanded through randomized rook neighborhood (refer to section 1.2. for details).	This study
S3	Random EEZ	Random placement of MPAs by Exclusive Economic Zone (EEZ) in proportion to the size of each country's maritime area.	62 initial cells making up 62 MPA patches randomly distributed in the EEZ of countries with a maritime territory > 400 km^2 in proportion to the size of the EEZ. MPAs were expanded by randomized rook neighborhood (refer to section 1.2. for details).	This study
S4	Micheli	Consensus areas among more than 5 proposed whole-basin conservation initiatives in the Mediterranean Sea.	62 initial cells placed according to priority consensus areas (see Supplementary Figure 4. 5). MPAs were expanded up to 10% coverage following the prioritization scheme, and up to 30% through randomized rook neighborhood, with the condition (when possible) that each new MPA cell be located within a consensus area (see Supplementary Figure 4. 4 for the extent of the consensus areas and refer to section 1.3. for details).	(35)
S5	Mazor-GFCM	Priority areas for conservation covering 10% of the distribution area of 77 threatened Mediterranean marine species while minimizing the fishing and aquaculture opportunity cost calculated for commercial fishing with GFCM-FAO data.	62 initial cells making up 62 MPA patches distributed across the 15 MPA patches of the scenario, consisting of cells that are more than 38% covered by a priority area, in proportion to the MPA patch size. MPAs were expanded up to 30% coverage through randomized rook neighborhood, with the condition (when possible) that each new MPA cell be located within a priority area (see Supplementary Figure 4. 4 for the extent of the priority areas and refer to section 1.3. for details).	(36)
S6	Mazor-SAUP	Priority areas for conservation covering 10% of the distribution area of 77 threatened Mediterranean marine species while minimizing the fishing and aquaculture opportunity cost calculated for commercial fishing with data from the Sea Around Us Project.	62 initial cells making up 62 MPAs distributed across the 40 MPA patches of the scenario, consisting of cells that are more than 38% covered by a priority area, in proportion to the MPA patch size. MPAs were expanded up to 30% coverage through randomized rook neighborhood, with the condition (when possible) that each new MPA cell be located within a priority area (see Supplementary Figure 4. 4 for the extent of the priority areas and refer to section 1.3. for details).	(36)

1.1. Scenario S1: Current network

The placement of initial MPAs in our baseline scenario was based on the current network of MPAs in the Mediterranean Sea from the MAPAMED database (37), considered to be the most complete database for MPAs in the Mediterranean Sea (38). Only areas with possible existing fishing regulations and that were prone to become fully protected areas (i.e., MPAs with a national statute, Marine Natura 2000 and Fisheries Restricted Areas) were selected. We excluded large-scale areas, such as the Pelagos Sanctuary covering 3.5% of the Mediterranean Sea or the deep-sea Fisheries Restricted Area covering 58.6% of the Mediterranean Sea, as we considered them too large to become no-take areas (Supplementary Table 4. 2). To avoid overestimating the total area covered by protection, overlapping protected areas were removed. Since protected areas that are only partially marine are present in the MAPAMED database, only the marine area of each MPA which overlapped the Mediterranean Sea shapefile polygon from IHO Sea Areas v3 (39) was retained. The resulting MPA network covered ca. 4.6% of the basin (113,577.3 km^2), representing 286 OSMOSE-MED grid cells and 62 MPA patches (Supplementary Figure 4. 2). Given the coarse spatial resolution of our model (20 x 20 km^2), this represented only cells more than 38% covered by an MPA. The same threshold was taken to determine the cells within the priority areas identified in scenarios S5-Mazor GFCM and S6-Mazor SAUP (see section 1.3).

To expand the current network up to 30% of the Mediterranean Sea, we first calculated the intersection between the OSMOSE-MED grid and the MPAs of our baseline network using QGIS 3.8 (see Supplementary Figure 4. 4, S1). Expansion of the network was done by randomized rook neighborhood, i.e. new MPA cells at each step were selected among the 4-neighbouring cells of each MPA patch. Up to 4.6% coverage (extent of the current MPA network considered), the expansion was constrained by the extent of the current network and new MPA cells were selected among the cells having the highest overlap percentage with predefined MPA zones. The expansion of the current network scenario (S1 – Current) served as a reference for all the other scenarios.

Supplementary Table 4. 2: MPA categories selected to constitute the baseline current Mediterranean MPA network.

MAPAMED category	Subcategories	Selection in study (YES – green, NO – red)	Justification
MPA	MPA with a national statute		Case-dependent but fishing regulations exist.
	Marine Natura 2000		Case-dependent but fishing regulations exist.
	Specially Protected Areas of Mediterranean Importance (SPAMI)		No fishing regulations.
Large-scale marine sanctuaries	Pelagos Sanctuary (3.5% of the Mediterranean Sea)		Driftnet ban for the protection of marine mammals only.
	Cetacean Migration Corridor (SPAMI) (1.8% of the Mediterranean Sea)		No fisheries regulations. Prohibition on underground geological research and hydrocarbon extraction only.
	OCEANID (pSCI) (0.3% of the Mediterranean Sea)		pSCI – not considered MPA yet.
Other Effective Conservation Measures (OECM)	Fisheries Restricted Areas – Vulnerable Marine Environments (FRA – VME)		Prohibition to use towed dredges and bottom trawl nets.
	Fisheries Restricted Areas – Essential Fish Habitats (FRA – EFH)		Temporal fishing closures, although regulation varies from one FRA to another.
	Deep-water FRA (58.6 % of the Mediterranean Sea) (classified as Site of Conservation Interest in the database)		Prohibition to use towed dredges and bottom trawl nets, but surface very large.
	Particularly Sensitive Area		Only marine traffic regulations.
Other sites of conservation interest	Ecologically or Biologically Significant Marine Areas (EBSAs)		Large areas with no fishing regulations.
	Ramsar sites		Conservation of wetlands.
	World Heritage Sites and Biosphere Reserves		International recognition without legal force.
	Cetaceans Critical Habitats (ACCOBAMS)		Identification of relevant areas, but no regulations.
Not integrated in the MAPAMED database	Important Marine Mammal areas		Identification of relevant areas, but no regulations.
	Marine Important Bid and Biodiversity Areas		Identification of relevant areas, but no regulations.
MPA coverage % of baseline current MPA network		4.6 %	

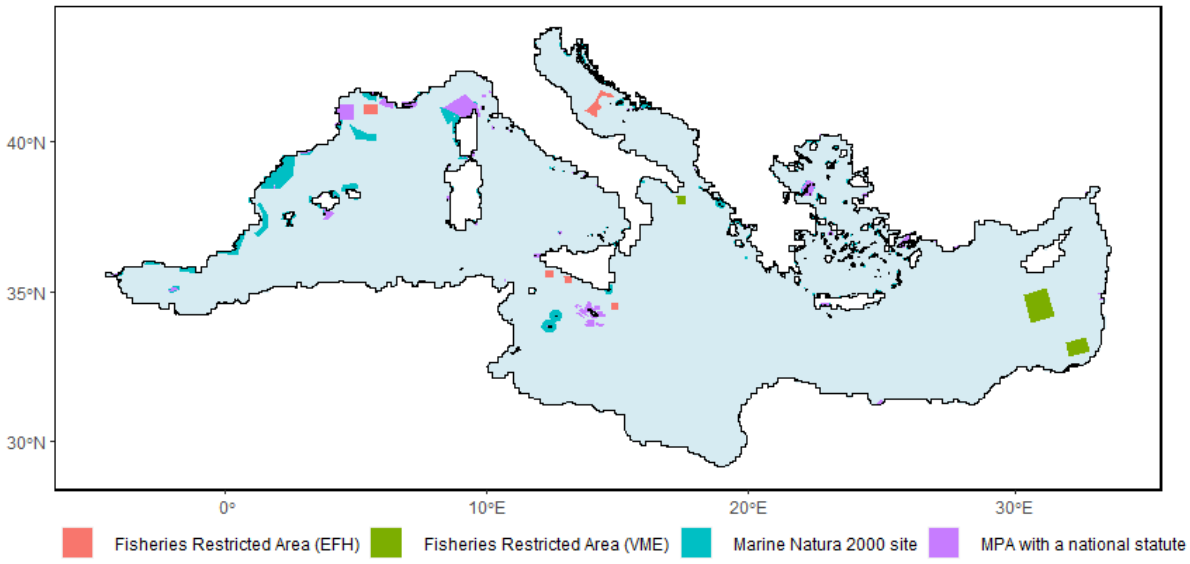

Supplementary Figure 4. 2: Initial current MPA network used as baseline, made up of Fisheries Restricted Areas (red and green), Marine Natura 2000 sites (blue) and MPAs with a national statute (purple).

1.2. Scenarios S2-S3: Random networks

We conceived two sets of random scenarios: one where MPAs were distributed randomly across the entire basin (S2 – Random basin) and one where MPAs were distributed by Economic Exclusive Zones in proportion to each country's maritime area (S3 – Random EEZ). Boundary of EEZ were taken from the (40). Only Mediterranean countries with a maritime territory 10 times larger than the minimum MPA size (determined by the model's spatial resolution, i.e., 400 km^2) were considered (**Error! Reference source not found.**3, Supplementary Figure 4. 3). Although this scenario may seem somewhat utopian at the scale of the Mediterranean basin, given the socio-political challenges in some countries and the fact that not all maritime areas in the Mediterranean Sea are universally recognized, it could still be easier to implement —at least in certain countries—compared to large-scale conservation plans involving transboundary MPAs. The expansion of the networks up to 30% of the Mediterranean Sea was done by randomized rook neighborhood.

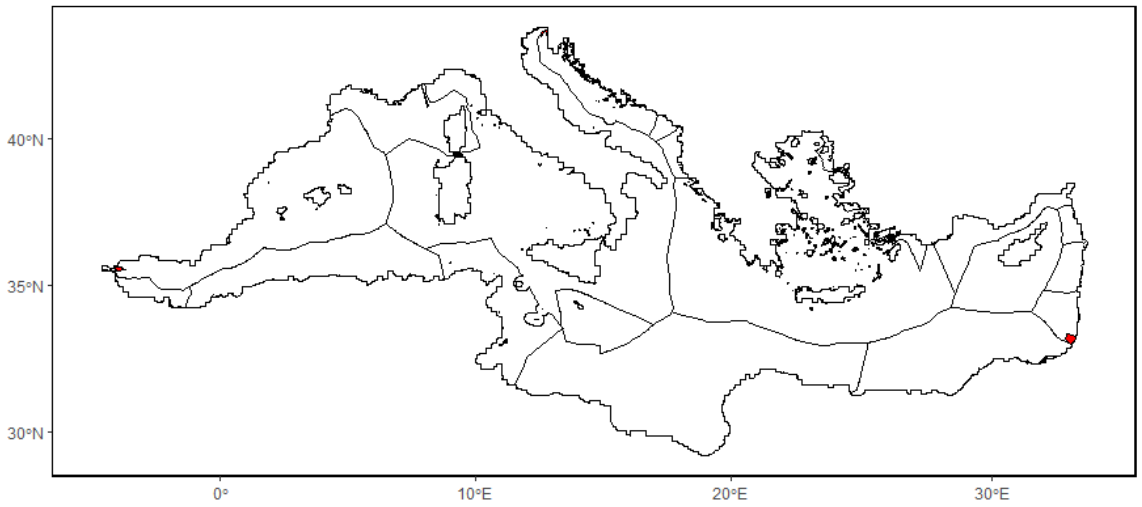

Supplementary Figure 4. 3: EEZ boundaries in the Mediterranean Sea. EEZs colored in red were not considered in our scenario because of their small size.

Supplementary Table 4. 3: Maritime areas in the Mediterranean Sea. Only 18 areas (shaded) belonging to 18 countries out of the 22 countries bordering the Mediterranean Sea were considered large enough to implement MPAs (minimum size of 400 km^2). No MPAs were implemented in Monaco, Bosnia and Herzegovina, Slovenia and Palestine as their EEZ were less than 10 times the minimum MPA size (EEZ < 4000 km^2). Areas claimed by more than one country were not considered.

Name	Status	Sovereign country 1	Sovereign country 2	Area* (km^2)
Overlapping claim Gibraltarian Exclusive Economic Zone	Overlapping claim	United Kingdom	Spain	388
Moroccan Exclusive Economic Zone	200NM	Morocco	NA	16911
Overlapping claim Melilla	Overlapping claim	Spain	Morocco	11
Overlapping claim Perejil Island	Overlapping claim	Spain	Morocco	1
Overlapping claim Ceuta	Overlapping claim	Spain	Morocco	33
Overlapping claim Chafarinas Islands	Overlapping claim	Spain	Morocco	26
Cypriote Exclusive Economic Zone	200NM	Cyprus	NA	96137
Egyptian Exclusive Economic Zone	200NM	Egypt	NA	169152
Lebanese Exclusive Economic Zone	200NM	Lebanon	NA	19777
Libyan Exclusive Economic Zone	200NM	Libya	NA	357776
Maltese Exclusive Economic Zone	200NM	Malta	NA	52925
Syrian Exclusive Economic Zone	200NM	Syria	NA	9835
Greek Exclusive Economic Zone	200NM	Greece	NA	465486
Turkish Exclusive Economic Zone	200NM	Turkey	NA	68561
Monégasque Exclusive Economic Zone	200NM	Monaco	NA	286
Tunisian Exclusive Economic Zone	200NM	Tunisia	NA	96020
Montenegrin Exclusive economic Zone	200NM	Montenegro	NA	6126
Albanian Exclusive Economic Zone	200NM	Albania	NA	11343
Palestinian Exclusive Economic Zone	200NM	Palestine	Israel	1088
Israeli Exclusive Economic Zone	200NM	Israel	NA	24035
Joint regime area Italy / France	Joint regime	France	Italy	67
Bosnian and Herzegovinian Exclusive Economic Zone	200NM	Bosnia and Herzegovina	NA	5
Croatian Exclusive Economic Zone	200NM	Croatia	NA	51689
Italian Exclusive Economic Zone	200NM	Italy	NA	519836
Slovenian Exclusive Economic Zone	200NM	Slovenia	NA	107
Joint regime area Croatia / Slovenia	Joint regime	Croatia	Slovenia	98
French Exclusive Economic Zone	200NM	France	NA	84099
Algerian Exclusive Economic Zone	200NM	Algeria	NA	127345
Spanish Exclusive Economic Zone	200NM	Spain	NA	255755

*Area in the Mediterranean Sea (CRS : 3035)

1.3. Scenarios S4-S6: Science-informed networks

We tested three scenarios from the scientific literature: a scenario where our initial protected areas corresponded to the conservation priority areas proposed by (41), based on the consensus among at least 5 proposed conservation initiatives in the Mediterranean Sea (S4 – Micheli); another scenario where the placement of MPAs was concordant with the conservation priority areas proposed by (36), protecting 10% of the distribution area of each of the 77 threatened marine species in the Mediterranean Sea (42), while considering explicitly a fishing and aquaculture opportunity cost calculated for commercial fishing with GFCM-FAO data (S5 – Mazor GFCM), and a last scenario, also proposed by (36), identical to the previous one but that used data from the Sea Around Us project to calculate the commercial fishing opportunity cost (S6 – Mazor SAUP).

For scenario S4-Micheli, we considered the prioritization proposed by (41) up to 10% coverage (Supplementary Figure 4. 5). Initial cells selected corresponded to the areas identified by the highest number of conservation initiatives in the Mediterranean Sea (Supplementary Figure 4. 5, in dark red). The further expansion of the network up to 30% of the Mediterranean Sea was done by randomized rook neighborhood, with two conditions: each new MPA cell had to be located within a consensus area (see Supplementary Figure 4. 4 for the extent of the consensus areas) and have the highest percentage of overlap with the consensus areas.

For scenario S5-Mazor GFCM, following the same methodology as for the current MPA network scenario (S1), we calculated the intersection between the OSMOSE-MED grid and the priority conservation areas of the scenario (scenario 8 in (36)) using QGIS 3.8, representing 600 OSMOSE-MED grid cells and 9.6% coverage (see Supplementary Figure 4. 4, S5). The first 62 cells to become MPAs (representing 1% of the total number of OSMOSE-MED grid cells), were selected from cells with more than 38% coverage by a priority area, representing 444 cells and 15 MPA patches, with two conditions: each cell had to form an MPA patch even if it was within the same MPA patch of a priority area, and have the highest percentage of overlap with priority areas. The network was extended through randomized rook neighborhood. Up to 9.6% coverage (the extent of the priority areas considered, see Supplementary Figure 4. 4), expansion was constrained by the extent of the priority areas and new MPA cells were selected from those cells with the highest percentage of overlap with the priority areas.

For scenario S6-Mazor SAUP, the same methodology as for scenario S5-Mazor GFCM was followed. We calculated the intersection between the OSMOSE-MED grid and the priority conservation areas of the scenario (scenario 9 in (36)) using QGIS 3.8, representing 892 OSMOSE-MED grid cells and 14.3% coverage (see Supplementary Figure 4. 4, S6). The first 62 cells to become MPAs (representing 1% of the total number of OSMOSE-MED grid cells), were selected from cells with more than 38% coverage by a priority area, representing 513 cells and 40 MPA patches, with two conditions: each cell had to form an MPA patch even if it was within the same MPA patch of a priority area, and have the highest percentage of overlap with priority areas. The network was extended through randomized rook neighborhood. Up to 14.3% coverage (the extent of the priority areas considered, see Supplementary Figure 4. 4), expansion was constrained by the extent of the priority areas and new MPA cells were selected from those cells with the highest percentage of overlap with the priority areas.

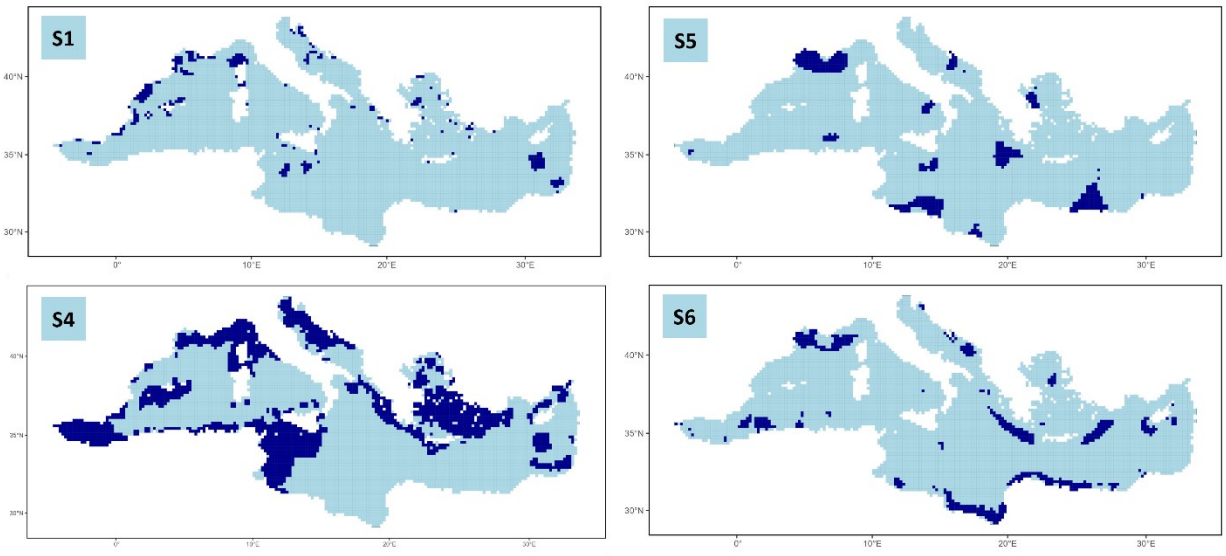

Supplementary Figure 4. 4: Intersection of the OSMOSE-MED grid and the areas selected in each scenario as potential MPA candidates. Refer to

for the description of the scenarios.

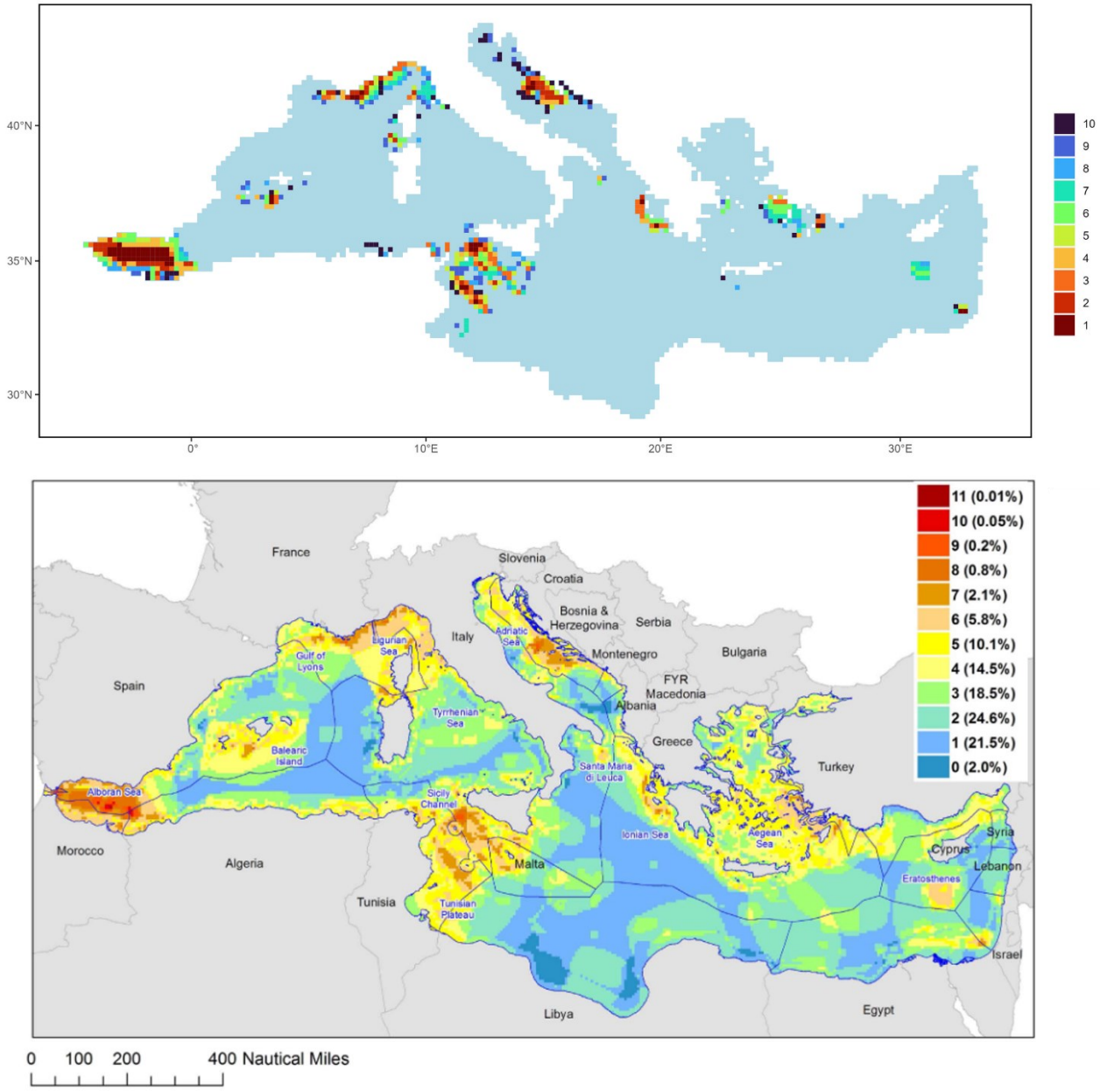

Supplementary Figure 4. 5: Selection of cells to be protected (top) following the prioritization scheme from (41) up to 10% coverage (bottom). The 62 initial selected cells are the cells in dark red (value = 1), which correspond with areas selected by the greatest number of conservation initiatives (in dark red, bottom).

Supplementary note 5: Model outputs - Total biomass and catch

1. Standard error of the mean of biomass and catch indicators according to the number of replicates and MPA coverage

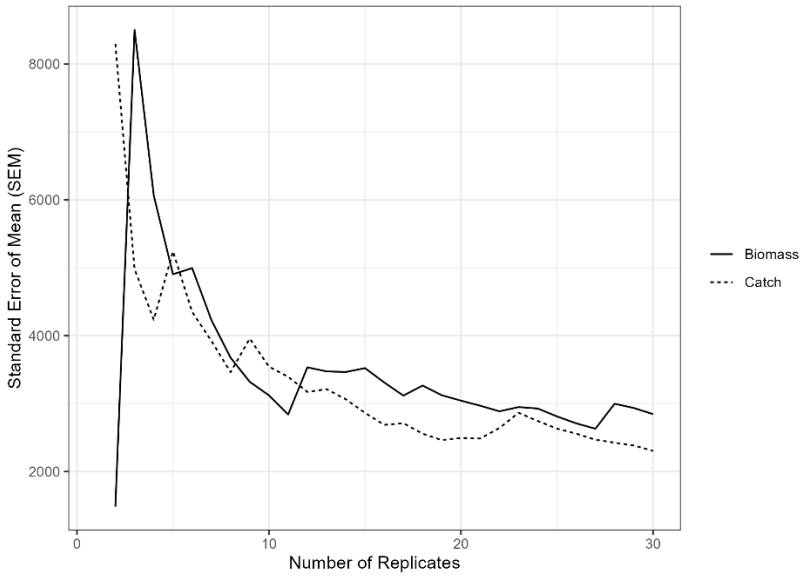

Supplementary Figure 5. 1: Standard error of the mean of total biomass and catch indicators according to the number of replicates in a scenario without MPAs. We see that > 20 replicates, the stochasticity inherent to the model stabilizes.

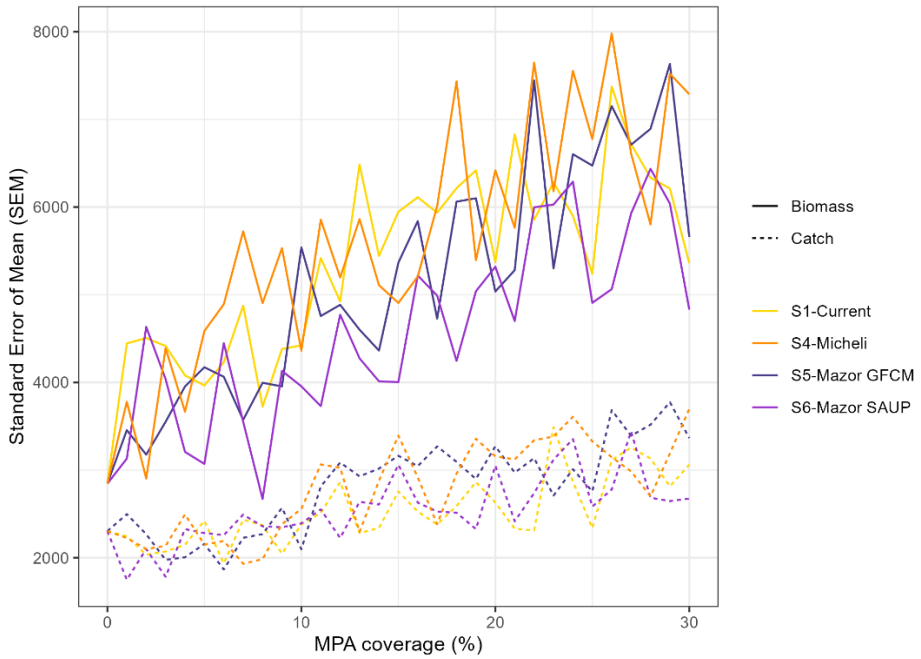

Supplementary Figure 5. 2: Standard error of the mean of total biomass and catch indicators with 30 replicates according to MPA coverage for MPA scenarios S1-Current, S4-Micheli, S5-Mazor GFCM and S6-Mazor SAUP with a proportional fishing redistribution strategy by GSA. We see that variability increases with MPA coverage especially for biomass.

2. Biomass and catch maps

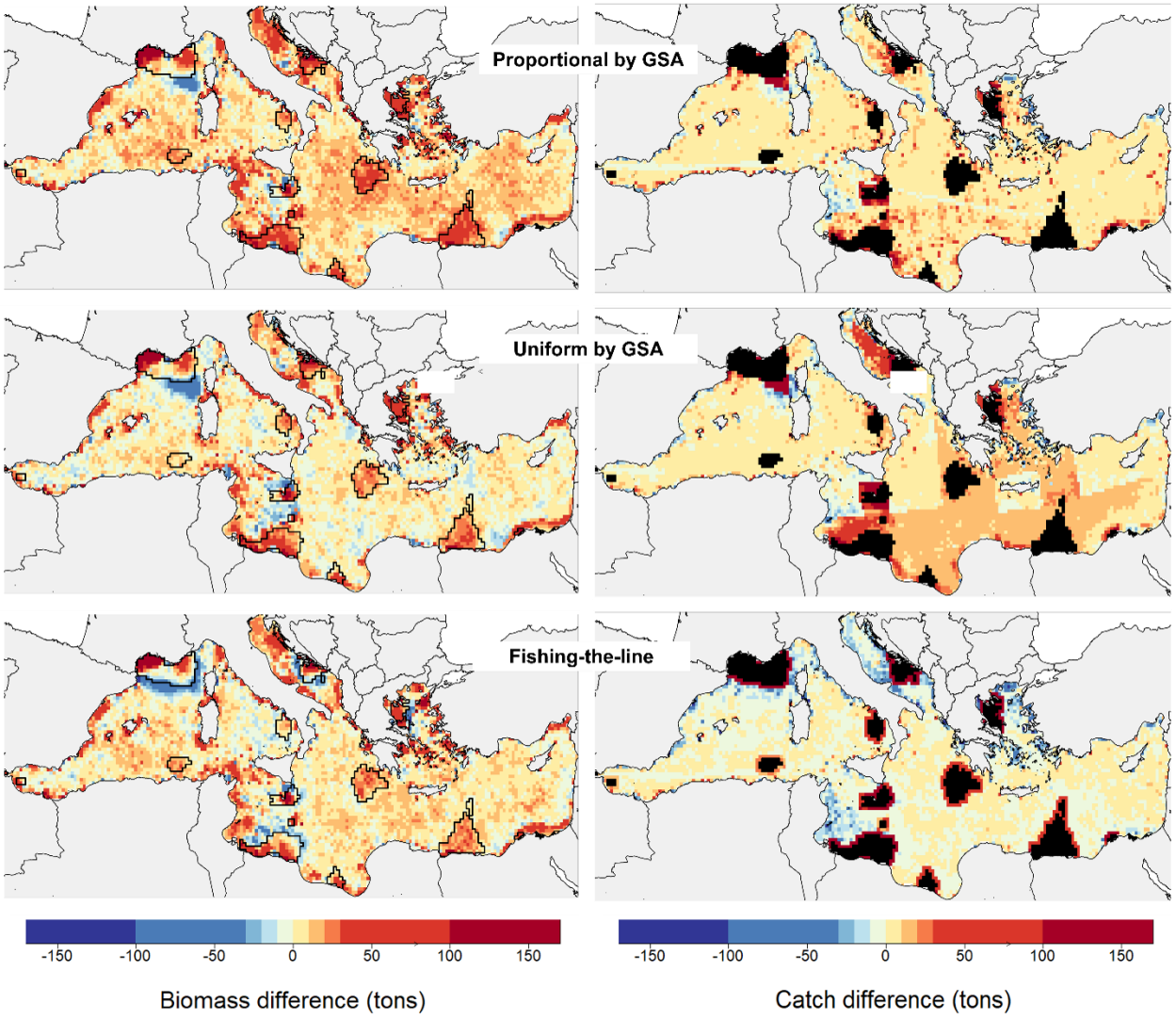

Supplementary Figure 5. 3: Difference in biomass and catch (in tons) before and after MPAs for the 3 different fishing redistribution strategies computed for the FPA scenario S5- Mazor GFCM at 10% coverage. MPAs are outlined in black for biomass change and shaded in black for catch difference.

Supplementary note 6: Model outputs - Biomass and catch by functional groups

1. List of species in OSMOSE-MED and associated group

Supplementary Table 6. 1: List of species in OSMOSE-MED. For the analysis in the present paper, species were grouped by their position in the water column (pelagic, demersal, benthic) and their size class (small, medium or large) calculated with the quantiles 0.33 and 0.66 of the species asymptotic lengths (LInf).

species_name	Linf (cm)	size_class	vertical_position	group
Alosa_alosa	70.3	Large	Pelagic	Large-sized pelagic fish
Alosa_fallax	52.1	Medium	Pelagic	Medium-sized pelagic fish
Anguilla_anguilla	70.18667	Large	Benthic	Large-sized benthic fish
Argyrosomus_regius	140	Large	Demersal	Large-sized demersal fish
Aristaeomorpha_foliacea	7.139	Small	Demersal	Crustacean
Aristeus_antennatus	7.433333	Small	Demersal	Crustacean
Atherina_boyeri	14.75	Small	Pelagic	Small-sized pelagic fish
Auxis_rochei_rochei	57.388	Large	Pelagic	Large-sized pelagic fish
Belone_belone	54.8	Medium	Pelagic	Medium-sized pelagic fish
Boops_boops	32.4	Medium	Demersal	Medium-sized demersal fish
Caranx_crysos	41.2	Medium	Pelagic	Medium-sized pelagic fish
Chelidonichthys_lucerna	55.05714	Large	Benthic	Large-sized benthic fish
Coris_julis	27.2	Small	Benthic	Small-sized benthic fish
Coryphaena_hippurus	101.45	Large	Pelagic	Large-sized pelagic fish
Crangon_crangon	7.79	Small	Benthic	Crustacean
Crystallogobius_linearis	5.4	Small	Benthic	Small-sized benthic fish
Dentex_dentex	90.625	Large	Demersal	Large-sized demersal fish
Dentex_gibbosus	107.24	Large	Demersal	Large-sized demersal fish
Dentex_maroccanus	34.9	Medium	Demersal	Medium-sized demersal fish
Dicentrarchus_labrax	69.62	Large	Demersal	Large-sized demersal fish
Diplodus_annularis	22.25249	Small	Demersal	Small-sized demersal fish
Diplodus_cervinus	68.8	Large	Demersal	Large-sized demersal fish
Diplodus_puntazzo	45.28	Medium	Demersal	Medium-sized demersal fish
Diplodus_sargus_sargus	44.2	Medium	Demersal	Medium-sized demersal fish
Diplodus_vulgaris	30.01778	Medium	Demersal	Medium-sized demersal fish

Eledone_cirrhosa	*19.28*	*Small*	*Benthic*	*Cephalopod*
Engraulis_encrasicolus	*18.408*	*Small*	*Pelagic*	*Small-sized pelagic fish*
Epinephelus_aeneus	*144.325*	*Large*	*Demersal*	*Large-sized demersal fish*
Epinephelus_marginatus	*137.4667*	*Large*	*Demersal*	*Large-sized demersal fish*
Etrumeus_teres	*33.77*	*Medium*	*Pelagic*	*Medium-sized pelagic fish*
Eutrigla_gurnardus	*46*	*Medium*	*Benthic*	*Medium-sized benthic fish*
Euphausiids	*1.84*	*Small*	*Pelagic*	*Crustacean*
Galeus_melastomus	*64*	*Large*	*Demersal*	*Large-sized demersal fish*
Gobius_niger	*15.9*	*Small*	*Benthic*	*Small-sized benthic fish*
Halobatrachus_didactylus	*52*	*Medium*	*Benthic*	*Medium-sized benthic fish*
Illex_coindetii	*29.63*	*Medium*	*Pelagic*	*Cephalopod*
Lepidorhombus_whiffiagonis	*44.8*	*Medium*	*Benthic*	*Medium-sized benthic fish*
Liza_aurata	*43.21431*	*Medium*	*Pelagic*	*Medium-sized pelagic fish*
Liza_ramada	*44.33501*	*Medium*	*Pelagic*	*Medium-sized pelagic fish*
Liza_saliens	*38.54452*	*Medium*	*Pelagic*	*Medium-sized pelagic fish*
Loligo_vulgaris	*23.8*	*Small*	*Demersal*	*Cephalopod*
Lophius_budegassa	*103*	*Large*	*Benthic*	*Large-sized benthic fish*
Lophius_piscatorius	*102*	*Large*	*Benthic*	*Large-sized benthic fish*
Merlangius_merlangus	*39.74833*	*Medium*	*Demersal*	*Medium-sized demersal fish*
Merluccius_merluccius	*105.4231*	*Large*	*Demersal*	*Large-sized demersal fish*
Micromesistius_poutassou	*49.3*	*Medium*	*Demersal*	*Medium-sized demersal fish*
Mugil_cephalus	*63.7*	*Large*	*Pelagic*	*Large-sized pelagic fish*
Mullus_barbatus_barbatus	*29.205*	*Small*	*Benthic*	*Small-sized benthic fish*
Mullus_surmuletus	*36.0225*	*Medium*	*Benthic*	*Medium-sized benthic fish*
Mustelus_mustelus	*175*	*Large*	*Demersal*	*Large-sized demersal fish*
Nephrops_norvegicus	*22.7*	*Small*	*Benthic*	*Crustacean*
Octopus_vulgaris	*29.6*	*Small*	*Benthic*	*Cephalopod*
Pagellus_acarne	*28.32414*	*Small*	*Demersal*	*Small-sized demersal fish*
Pagellus_erythrinus	*37.35059*	*Medium*	*Demersal*	*Medium-sized demersal fish*
Pagrus_pagrus	*63.96*	*Large*	*Demersal*	*Large-sized demersal fish*
Palaemon_serratus	*8.596*	*Small*	*Benthic*	*Crustacean*
Palinurus_elephas	*17.85*	*Small*	*Benthic*	*Crustacean*
Parapenaeus_longirostris	*4.438643*	*Small*	*Demersal*	*Crustacean*
Penaeus_kerathurus	*18.03*	*Small*	*Benthic*	*Crustacean*

Phycis_phycis	*67.15*	*Large*	*Benthic*	*Large-sized benthic fish*
Platichthys_flesus_flesus	*38.5*	*Medium*	*Benthic*	*Medium-sized benthic fish*
Pleuronectes_platessa	*55.635*	*Large*	*Benthic*	*Large-sized benthic fish*
Pomatomus_saltatrix	*111.2008*	*Large*	*Pelagic*	*Large-sized pelagic fish*
Pomatoschistus_marmoratus	*6.453252*	*Small*	*Benthic*	*Small-sized benthic fish*
Pomatoschistus_minutus	*8.15*	*Small*	*Benthic*	*Small-sized benthic fish*
Rhinobatos_rhinobatos	*128.6*	*Large*	*Benthic*	*Large-sized benthic fish*
Sarda_sarda	*82.38*	*Large*	*Pelagic*	*Large-sized pelagic fish*
Sardina_pilchardus	*21.30167*	*Small*	*Pelagic*	*Small-sized pelagic fish*
Sardinella_aurita	*27.5375*	*Small*	*Pelagic*	*Small-sized pelagic fish*
Saurida_undosquamis	*41.765*	*Medium*	*Demersal*	*Medium-sized demersal fish*
Sciaena_umbra	*54.05*	*Medium*	*Demersal*	*Medium-sized demersal fish*
Scomber_colias	*39.925*	*Medium*	*Pelagic*	*Medium-sized pelagic fish*
Scomber_scombrus	*37.3*	*Medium*	*Pelagic*	*Medium-sized pelagic fish*
Scophthalmus_maximus	*63.06364*	*Large*	*Benthic*	*Large-sized benthic fish*
Scorpaena_notata	*16.925*	*Small*	*Benthic*	*Small-sized benthic fish*
Scyliorhinus_canicula	*56.8*	*Large*	*Demersal*	*Large-sized demersal fish*
Sepia_officinalis	*28.38333*	*Small*	*Demersal*	*Cephalopod*
Seriola_dumerili	*174.6*	*Large*	*Pelagic*	*Large-sized pelagic fish*
Serranus_atricauda	*49.5*	*Medium*	*Demersal*	*Medium-sized demersal fish*
Solea_solea	*39.6*	*Medium*	*Benthic*	*Medium-sized benthic fish*
Sparus_aurata	*57.03333*	*Large*	*Demersal*	*Large-sized demersal fish*
Sphyraena_sphyraena	*55.3*	*Large*	*Pelagic*	*Large-sized pelagic fish*
Sphyraena_viridensis	*100.6*	*Large*	*Pelagic*	*Large-sized pelagic fish*
Spicara_maena	*21.99*	*Small*	*Demersal*	*Small-sized demersal fish*
Spicara_smaris	*19.6*	*Small*	*Pelagic*	*Small-sized pelagic fish*
Spondyliosoma_cantharus	*41.7*	*Medium*	*Demersal*	*Medium-sized demersal fish*
Sprattus_sprattus	*14.29571*	*Small*	*Pelagic*	*Small-sized pelagic fish*
Squilla_mantis	*19.69*	*Small*	*Benthic*	*Crustacean*
Stephanolepis_diaspros	*27.83*	*Small*	*Demersal*	*Small-sized demersal fish*
Thunnus_alalunga	*94.7*	*Large*	*Pelagic*	*Large-sized pelagic fish*
Thunnus_thynnus	*319*	*Large*	*Pelagic*	*Large-sized pelagic fish*
Trachurus_mediterraneus	*35.20909*	*Medium*	*Pelagic*	*Medium-sized pelagic fish*
Trachurus_picturatus	*62.7*	*Large*	*Pelagic*	*Large-sized pelagic fish*

Trachurus_trachurus	*32.2645*	*Medium*	*Pelagic*	*Medium-sized pelagic fish*
Trachyrincus_scabrus	*47.75*	*Medium*	*Demersal*	*Medium-sized demersal fish*
Trigla_lyra	*61.46626*	*Large*	*Benthic*	*Large-sized benthic fish*
Trisopterus_luscus	*44.375*	*Medium*	*Demersal*	*Medium-sized demersal fish*
Trisopterus_minutus	*25.94286*	*Small*	*Demersal*	*Small-sized demersal fish*
Upeneus_moluccensis	*25.69761*	*Small*	*Demersal*	*Small-sized demersal fish*
Xiphias_gladius	*238.5*	*Large*	*Pelagic*	*Large-sized pelagic fish*
Zosterisessor_ophiocephalus	*27.4*	*Small*	*Benthic*	*Small-sized benthic fish*

2. Predation pressure on low-trophic level species

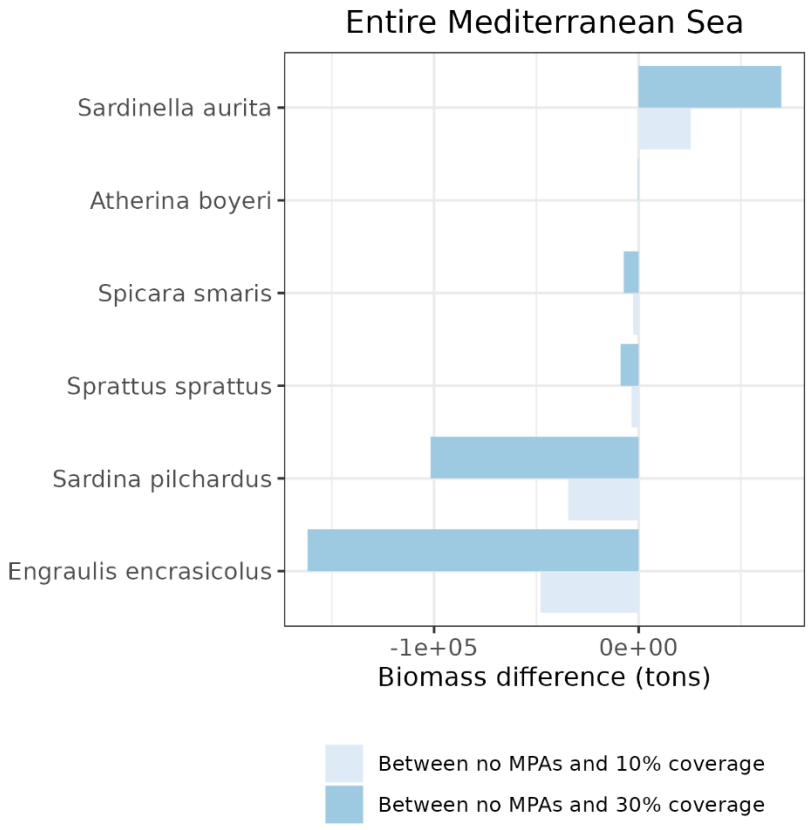

Supplementary Figure 6. 1: Small pelagic species biomass difference in tons for a 10% and 30% MPA coverage, relative to a scenario without MPAs for the scenario S5-Mzaor GFCM. Differences are calculated over the entire Mediterranean Sea.

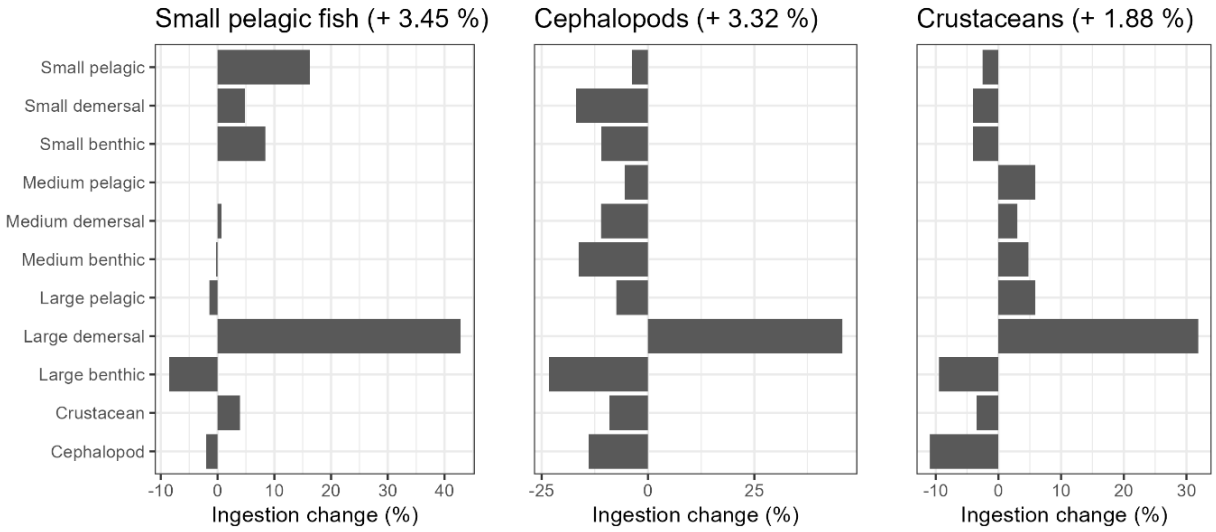

Supplementary Figure 6. 2: Predation pressure change by functional groups on main low-trophic level groups (small pelagic fish, cephalopods, crustaceans) between before and after fully protecting 10% of the Mediterranean Sea. Total predation pressure change is indicated in the plot title. The analysis is made on scenario "S5-Mazor GFCM", considering fishers redistribute proportionally to the spatial distribution of fishing effort prior to no-take MPA establishment by geographical sub-area (GSA).

3. Other scenarios

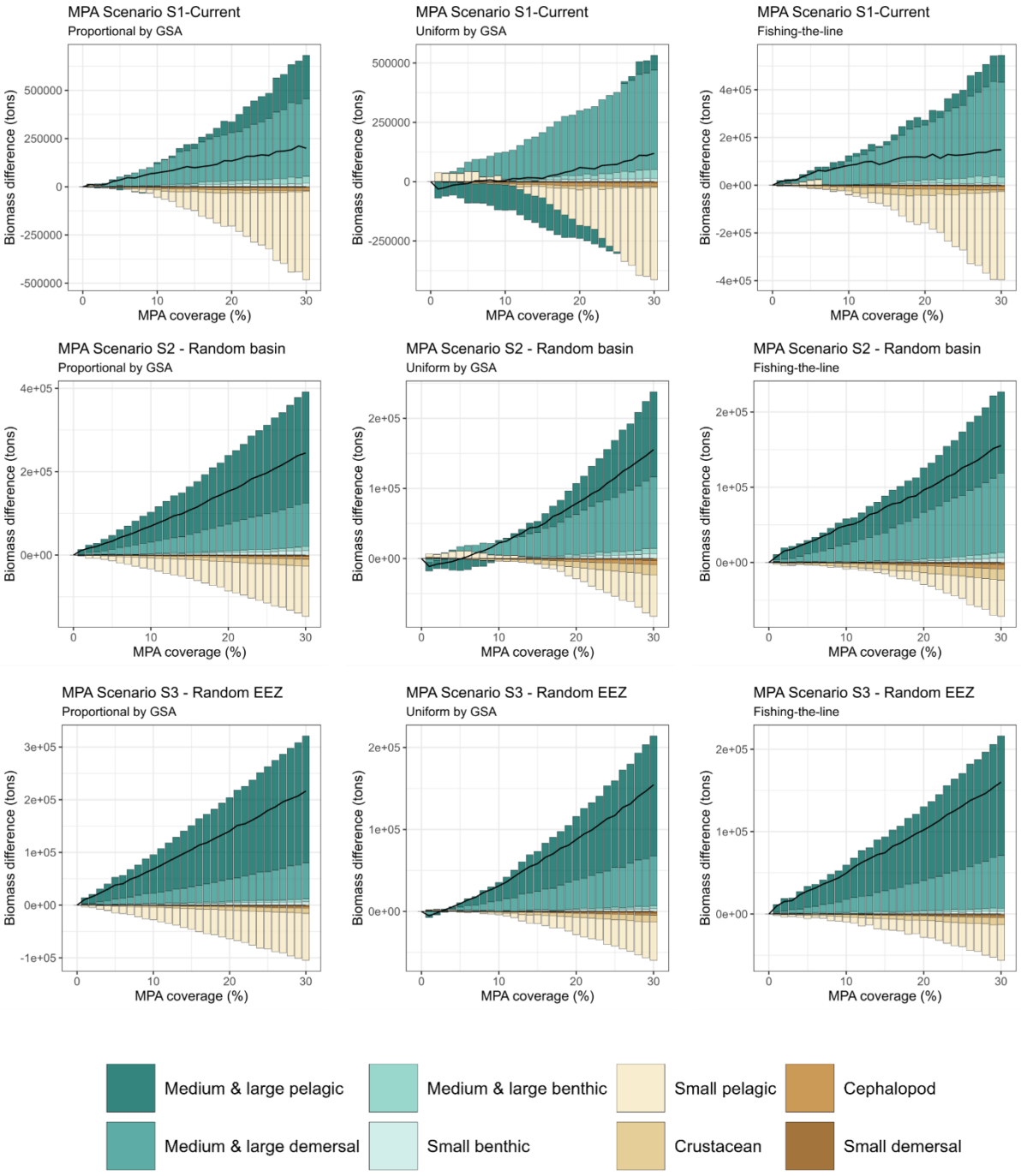

Supplementary Figure 6. 3: Biomass changes by groups and fishing redistribution strategies for MPA scenarios S1, S2 and S3.

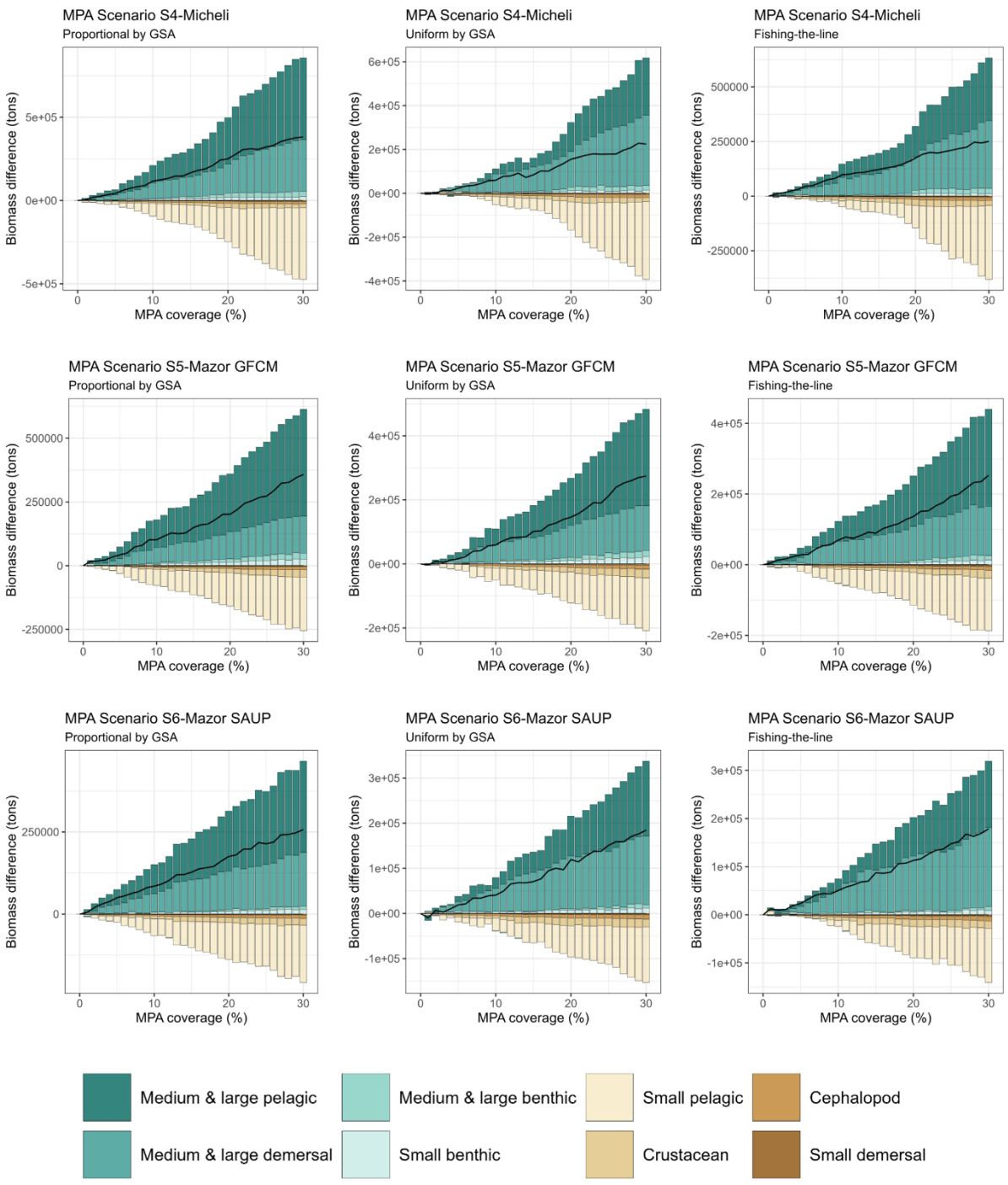

Supplementary Figure 6. 4: Biomass changes by groups and fishing redistribution strategies for MPA scenarios S4, S5 and S6.

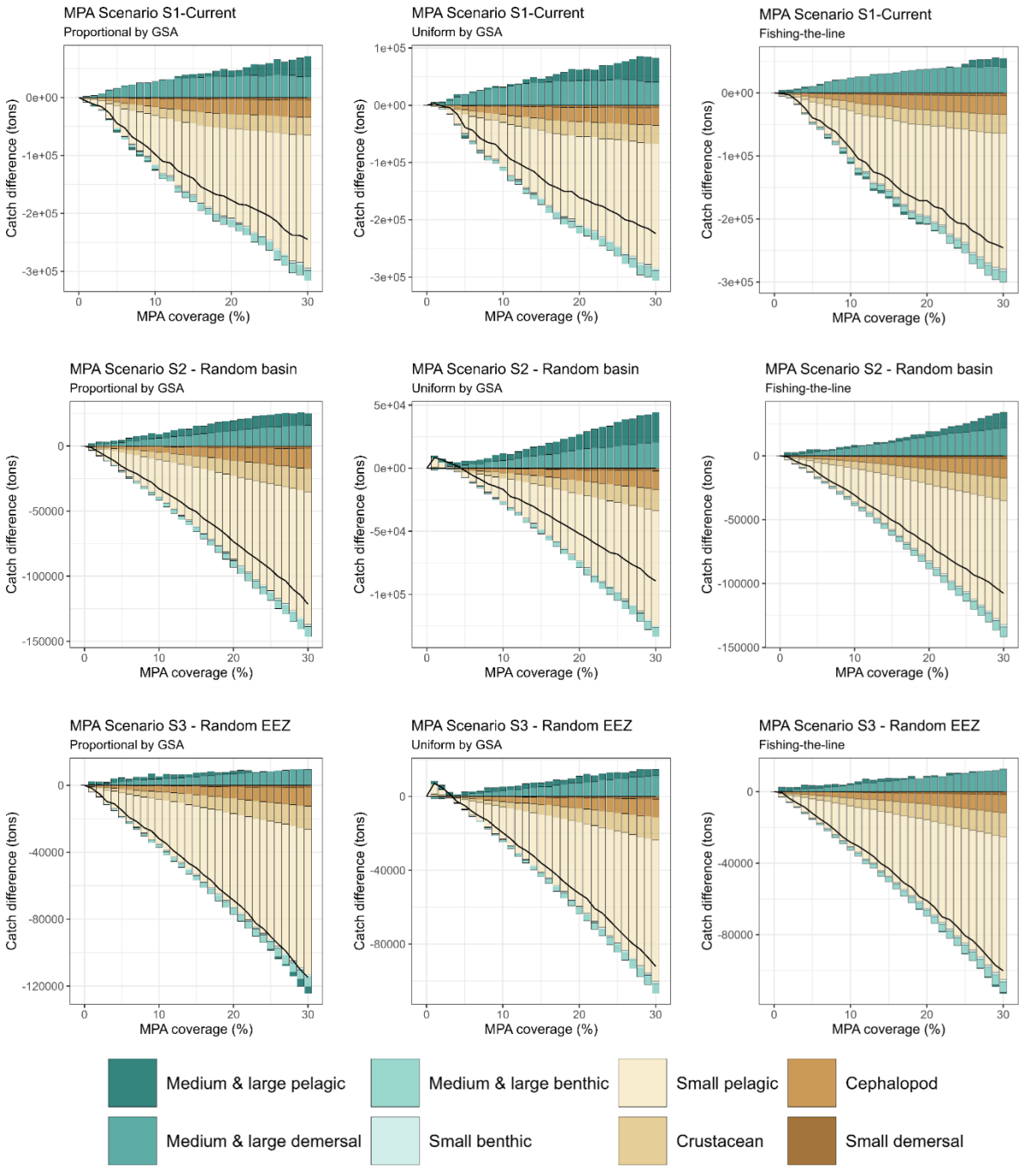

Supplementary Figure 6. 5: Catch changes by groups and fishing redistribution strategies for MPA scenarios S1, S2 and S3.

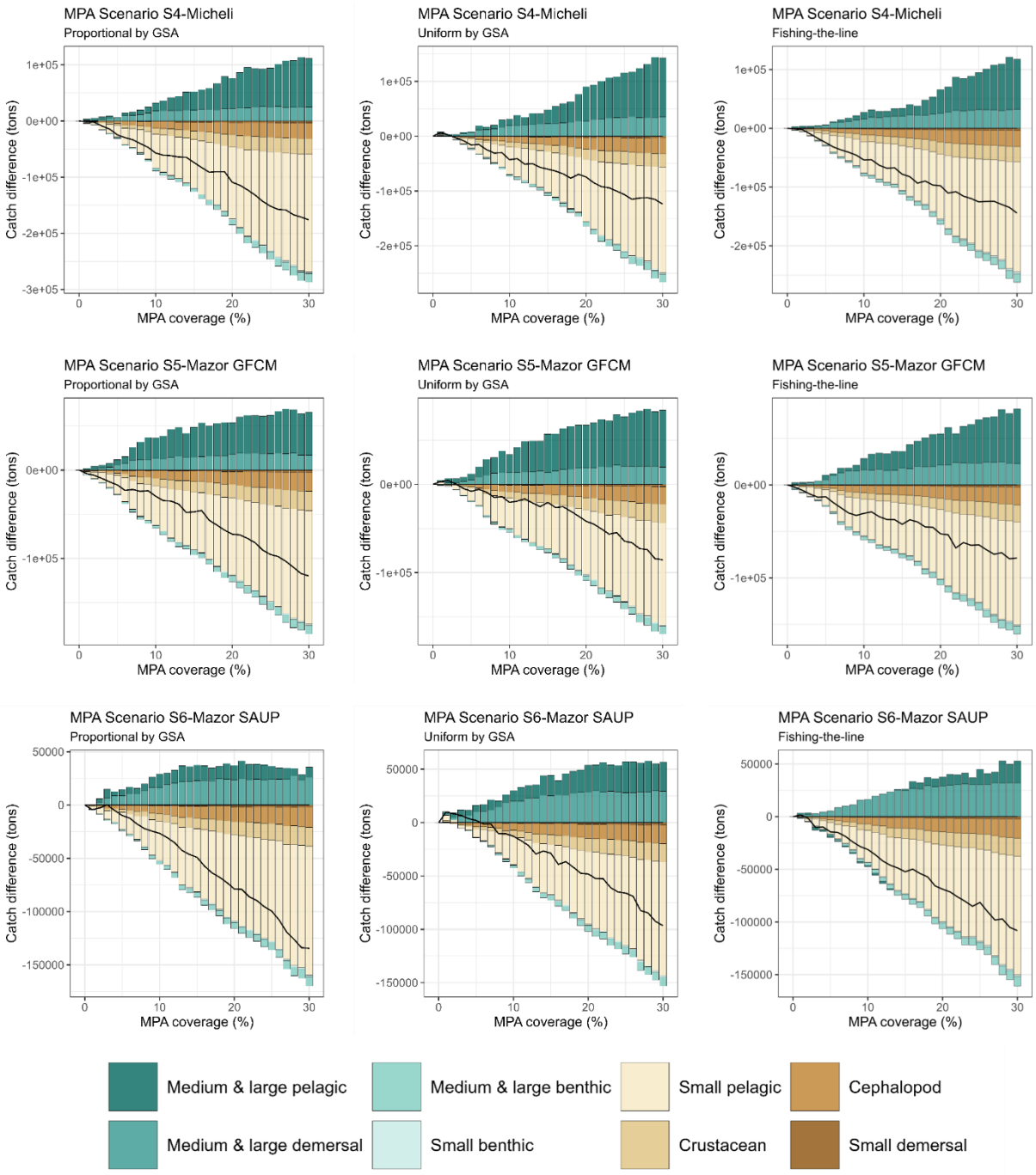

Supplementary Figure 6. 6: Catch changes by groups and fishing redistribution strategies for MPA scenarios S4, S5 and S6.

Supplementary note 7: Model outputs – Hill-Shannon diversity

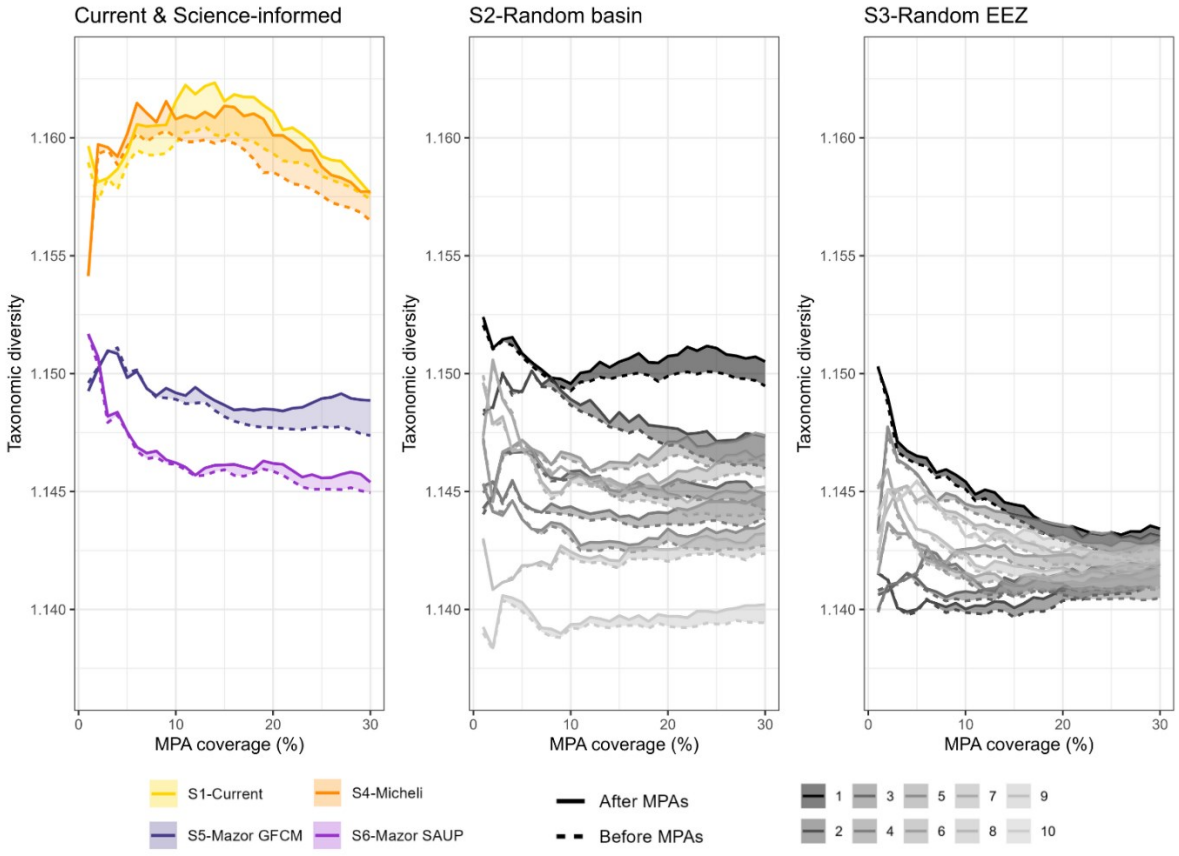

Supplementary Figure 7. 1: Taxonomic α-diversity inside FPAs before and after their establishment calculated with the Hill-Shannon diversity index exponentiated (Hill number of order q = 1). Species are weighted in proportion to their abundances. The shaded envelope represents the change of taxonomic α-diversity due to FPAs. Variability due to the model's inherent stochasticity is not shown, as it is assumed to be stable when averaging 30 replicates (refer to Supplementary Figure 5. 1).

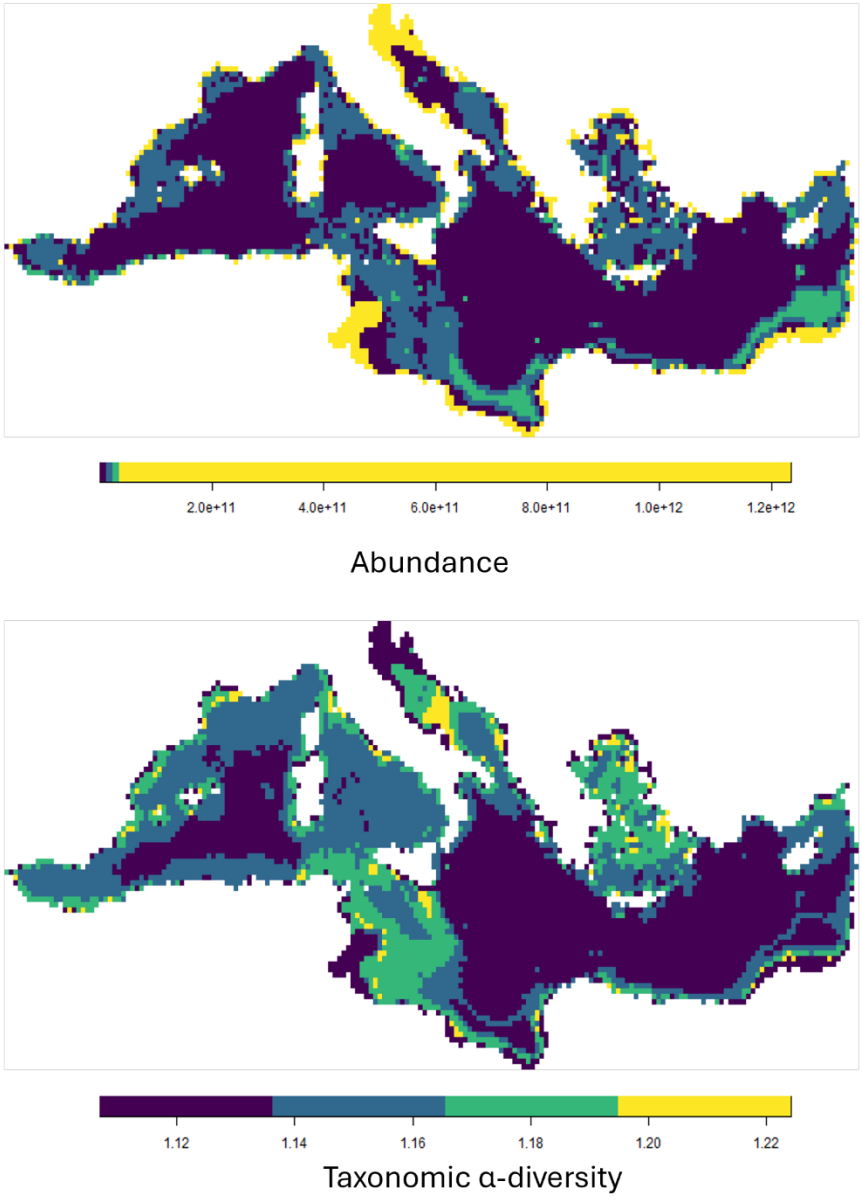

Supplementary Figure 7. 2: Total species abundance and taxonomic α-diversity distribution across the Mediterranean Sea before MPA establishment. We see that α-diversity is highest closer to the coast, except in some coastal areas, where total abundance is very high (e.g., Gulf of Gabès, northern Adriatic Sea).

Supplementary note 8: Redundancy Analysis

Supplementary Table 8. 1: Description of shape metrics from the R package Landscapemetrics selected in the Redundancy Analysis (RDA).

METRIC NAME	TYPE OF METRIC	BEHAVIOUR	FORMULA
Number of patches (np)	Aggregation	Inversely related to mean patch size for a given coverage	
Percentage of like adjacencies (pladj)	Aggregation	Level of aggregation of the network. PLADJ = 0 if class *i* is maximal disaggregated, i.e. every cell is a different patch. PLADJ = 100 when the only one patch is present.	$PLADJ = \left(\frac{g_{ij}}{\sum_{k=1}^{m} g_{ik}}\right) x\ 100$, where g_{ij} is the number of adjacencies between cells of class i and j and g_{ik} is the number of adjacencies between cells of class i and k.
Mean shape index (shape_mn)	Shape	Inverse of the mean patch compactness of the network. The shape index of each patch (SHAPE) is the ratio between the actual perimeter of the patch and the hypothetical minimum perimeter of the patch. The minimum perimeter equals the perimeter if the patch would be maximally compact.	$SHAPE_{CV} = mean(SHAPE[patch_{ij}])$, where $SHAPE[patch_{ij}]$ is the shape index of each patch.
Distance to coast (distance_to_coast)	Shape	Distance to coast is calculated by MPA patch from the centroid of the patch to the nearest land cell and averaged over the entire network between patches.	

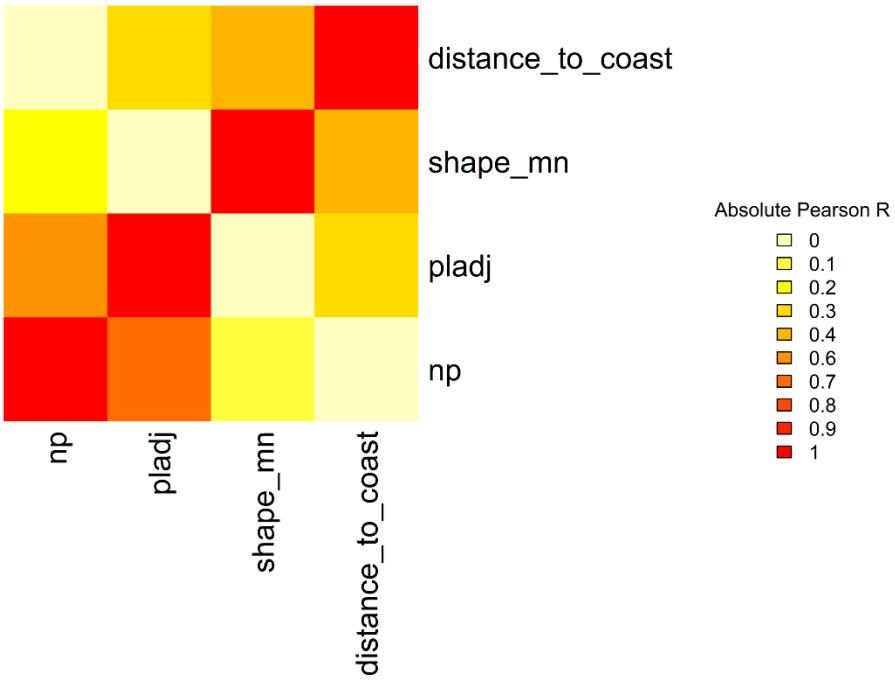

Supplementary Figure 8. 1: Heatmap representing the absolute Pearson correlation R between explanatory variables used in the Redundancy Analysis (RDA).

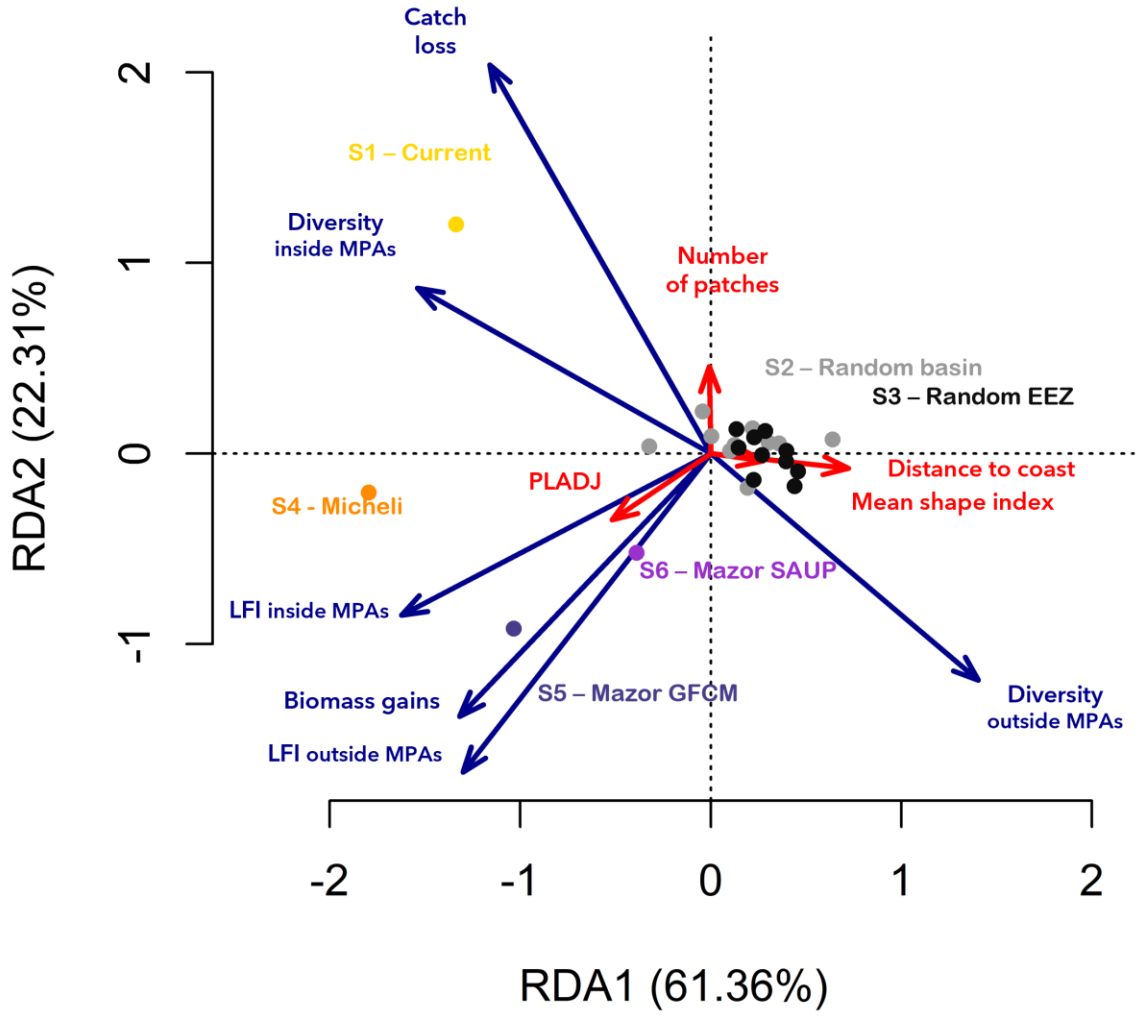

Supplementary Figure 8. 2: Redundancy Analysis (RDA) (using scaling 1) showing the structural differences between FPA networks S1 to S6 (dots). Under scaling 1, the angle between response (blue arrows) and explanatory variables (red arrows) reflect their correlations but not the angles between themselves. The projection of a scenario (dots S1 to S6) at right angle on a response or an explanatory variable approximates the value of this scenario along that variable. The distances between scenario projections (dots) approximate their Euclidian distances.

References

1. F. Moullec, *et al.*, Capturing the big picture of Mediterranean marine biodiversity with an end-to-end model of climate and fishing impacts. *Prog. Oceanogr.* **178**, 102179 (2019).

2. F. Sevault, *et al.*, A fully coupled Mediterranean regional climate system model: design and evaluation of the ocean component for the 1980–2012 period. *Tellus Dyn. Meteorol. Oceanogr.* **66**, 23967 (2014).

3. A. Voldoire, *et al.*, The CNRM-CM5.1 global climate model: description and basic evaluation. *Clim. Dyn.* **40**, 2091–2121 (2013).

4. P. A. Auger, *et al.*, Functioning of the planktonic ecosystem on the Gulf of Lions shelf (NW Mediterranean) during spring and its impact on the carbon deposition: a field data and 3-D modelling combined approach. *Biogeosciences* **8**, 3231–3261 (2011).

5. T. R. Anderson, P. Pondaven, Non-redfield carbon and nitrogen cycling in the Sargasso Sea: pelagic imbalances and export flux. *Deep Sea Res. Part Oceanogr. Res. Pap.* **50**, 573–591 (2003).

6. C. Raick, E. J. M. Delhez, K. Soetaert, M. Grégoire, Study of the seasonal cycle of the biogeochemical processes in the Ligurian Sea using a 1D interdisciplinary model. *J. Mar. Syst.* **55**, 177–203 (2005).

7. F. Kessouri, "Cycles biogéochimiques de la mer Méditerranée : processus et bilans," Toulouse 3. (2015).

8. C. Ulses, *et al.*, Budget of organic carbon in the North-Western Mediterranean open sea over the period 2004-2008 using 3-D coupled physical-biogeochemical modeling. *J. Geophys. Res. Oceans* **121**, 7026 (2016).

9. C. Piroddi, M. Coll, J. Steenbeek, D. Macías, V. Christensen, Modelling the Mediterranean marine ecosystem as a whole: addressing the challenge of complexity. *Mar. Ecol. Prog. Ser.* **533**, 47–65 (2015).

10. Y.-J. Shin, P. Cury, Using an individual-based model of fish assemblages to study the response of size spectra to changes in fishing. *Can. J. Fish. Aquat. Sci.* **61**, 414–431 (2004).

11. V. Christensen, C. J. Walters, Ecopath with Ecosim: methods, capabilities and limitations. *Ecol. Model.* **172**, 109–139 (2004).

12. Y.-J. Shin, P. Cury, Exploring fish community dynamics through size-dependent trophic interactions using a spatialized individual-based model. *Aquat. Living Resour.* **14**, 65–80 (2001).

13. M. Travers, *et al.*, Two-way coupling versus one-way forcing of plankton and fish models to predict ecosystem changes in the Benguela. *Ecol. Model.* **220**, 3089–3099 (2009).

14. C. Albouy, *et al.*, FishMed: traits, phylogeny, current and projected species distribution of Mediterranean fishes, and environmental data. *Ecology* **96**, 2312–2313 (2015).

15. W. Thuiller, B. Lafourcade, R. Engler, M. B. Araújo, BIOMOD – a platform for ensemble forecasting of species distributions. *Ecography* **32**, 369–373 (2009).

16. T. Hattab, *et al.*, The Use of a Predictive Habitat Model and a Fuzzy Logic Approach for Marine Management and Planning. *PLOS ONE* **8**, e76430 (2013).

17. O. Allouche, A. Tsoar, R. Kadmon, Assessing the accuracy of species distribution models: prevalence, kappa and the true skill statistic (TSS). *J. Appl. Ecol.* **43**, 1223–1232 (2006).

18. S. Drira, *et al.*, Species' climate niche modeling framework Predicting historical & future species' spatial distributions & estimation of species' thermal tolerance. (2023). https://doi.org/10.5281/zenodo.7646699.

19. R. Oliveros-Ramos, Y. Shin, calibrar: An R package for fitting complex ecological models. *Methods Ecol. Evol.* **16**, 507–519 (2025).

20. R. Oliveros-Ramos, P. Verley, V. Echevin, Y.-J. Shin, A sequential approach to calibrate ecosystem models with multiple time series data. *Prog. Oceanogr.* **151**, 227–244 (2017).

21. Pauly and Zeller, D. Pauly and D. Zeller, editors. 2015. Catch Reconstruction: concepts, methodss and data sources. Online Publication. Sea Around Us (www.seaaroundus.org). University of British Columbia. Deposited 2015.

22. P. K. Karachle, K. I. Stergiou, An update on the feeding habits of fish in the Mediterranean Sea (2002-2015). *Mediterr. Mar. Sci.* **18**, 43–52 (2017).

23. K. I. Stergiou, V. S. Karpouzi, Feeding habits and trophic levels of Mediterranean fish. *Rev. Fish Biol. Fish.* **11**, 217–254 (2002).

24. FAO, *The State of Mediterranean and Black Sea Fisheries 2023: Special edition* (FAO, 2023).

25. FAO, *The State of Mediterranean and Black Sea Fisheries 2022* (FAO, 2022).

26. B. Öztürk, Nature and extent of the illegal, unreported and unregulated (IUU) fishing in the Mediterranean Sea. 25 (2015).

27. C. Santamaria, *et al.*, Mass Processing of Sentinel-1 Images for Maritime Surveillance. *Remote Sens.* **9**, 678 (2017).

28. Copernicus, Copernicus Sentinel Data 2019. Available at: https:// search.asf.alaska.edu/#/. (2022).

29. JRC, *The SUMO ship detection software for satellite radar images h [er] :short installation and user guide*. (Publications Office, 2017).

30. H. Greidanus, *et al.*, The SUMO Ship Detector Algorithm for Satellite Radar Images. *Remote Sens.* **9**, 246 (2017).

31. A. Galdelli, A. Mancini, C. Ferrà, A. N. Tassetti, A Synergic Integration of AIS Data and SAR Imagery to Monitor Fisheries and Detect Suspicious Activities. *Sensors* **21**, 2756 (2021).

32. I. Pita, *et al.*, SAR Satellite Imagery Reveals the Impact of the Covid-19 Crisis on Ship Frequentation in the French Mediterranean Waters. *Front. Mar. Sci.* **9** (2022).

33. B. S. Halpern, *et al.*, Spatial and temporal changes in cumulative human impacts on the world's ocean. *Nat. Commun.* **6**, 7615 (2015).

34. D. A. Kroodsma, *et al.*, Tracking the global footprint of fisheries. *Science* **359**, 904–908 (2018).

35. F. Micheli, *et al.*, Setting Priorities for Regional Conservation Planning in the Mediterranean Sea. *PLoS ONE* **8**, e59038 (2013).

36. T. Mazor, S. Giakoumi, S. Kark, H. P. Possingham, Large-scale conservation planning in a multinational marine environment: cost matters. *Ecol. Appl.* **24**, 1115–1130 (2014).

37. MedPAN/SPARAC-MAPAMED. (2019). Available at: https://www.mapamed.org/ [Accessed 19 July 2022].

38. J. Claudet, C. Loiseau, M. Sostres, M. Zupan, Underprotected Marine Protected Areas in a Global Biodiversity Hotspot. *One Earth* **2**, 380–384 (2020).

39. Flanders Marine Institute (VLIZ), IHO Sea Areas, version 3. Marine Data Archive. https://doi.org/10.14284/323. Deposited 2018.

40. Flanders Marine Institute, The union of world country boundaries and EEZ's, version 3. Marine Data Archive. https://doi.org/10.14284/403. Deposited 2020.

41. F. Micheli, *et al.*, Setting Priorities for Regional Conservation Planning in the Mediterranean Sea. *PLoS ONE* **8**, e59038 (2013).

42. T. Mazor, H. P. Possingham, S. Kark, Collaboration among countries in marine conservation can achieve substantial efficiencies. *Divers. Distrib.* **19**, 1380–1393 (2013).